Summer 8-5-2013

Relaxation of Shear-Induced Precursors in Isotactic Polypropylene and Random Propylene-Ethylene copolymers

Benjamin Schammé
University of Nebraska-Lincoln, benjamin.schamme@gmail.com

RELAXATION OF SHEAR-INDUCED PRECURSORS IN ISOTACTIC POLYPROPYLENE AND RANDOM PROPYLENE-ETHYLENE COPOLYMERS

By

Benjamin Schammé

A THESIS

Presented to the Faculty of

The Graduate College at the University of Nebraska

In Partial Fulfillment of the Requirements

For the Degree of Master of Science

Major: Mechanical Engineering and Applied Mechanics

Under the Supervision of Lucia Fernandez-Ballester

Lincoln, Nebraska

August, 2013

RELAXATION OF SHEAR-INDUCED PRECURSORS IN ISOTACTIC POLYPROPYLENE AND RANDOM PROPYLENE-ETHYLENE COPOLYMERS

Benjamin Schammé, M.S

University of Nebraska, 2013

Adviser: Lucia Fernandez-Ballester

Flow induced crystallization (FIC) has a large impact on kinetics and morphology of semicrystalline polymers, and can therefore drastically change final properties such as dimensional and thermal stability, modulus and strength. Processing of polymers usually involves flow, so it is important to understand the mechanism of FIC. It is known that oriented precursors formed during flow are the key to FIC but they are not yet well understood. In this study, flow induced precursors are investigated by examining their relaxation, and the effect of comonomer is probed.

Using a commercial isotactic polypropylene and random propylene-ethylene copolymers, a fiber pull-out technique coupled with polarized optical microscope and a hot stage has been used, as in terms of sensitivity is the most powerful indicator of melt perturbations. The distinct morphological zones that happen after shear and relaxation (cylindritic or highly nucleated morphology and classical spherulitic morphology) have been used as an

indicator of whether full reequilibration has been attained or not in the sheared melt. The lifetime of precursors, t*, has been associated with the full disappearance of cylindritic morphology. Data of t* obtained in a range of relaxation temperatures were fitted with an Arrhenius-type equation leading to values of apparent activation energy and detaching stem length. The apparent energies of activation E_a for disappearance of precursors and stem detaching length L_S were found to decrease with increasing ethylene content. The values of E_a for iPP in this study were somewhat larger than those in the literature. The possible reasons for such differences are discussed. The values of L_S were within the range previously found for other semicrystalline polymers.

ACKNOWLEDGEMENT

I would like to express my gratitude to the following persons for their constant support throughout this project. Dr. Lucia Fernandez-Ballester for her encouragement, supervision and insightful comments and suggestions. Without her guidance, this thesis would not have been possible. Professor Jean-Marc Saiter, Professor Mehrdad Negahban and the staff of the both universities (University of Rouen and UNL) whom allowed the exchange becomes possible. I would also like to thank Frederic Aubin for his help during all these year. I finally would like to thank my family who has been supportive over my university education and my entire life. Without forgetting my second family with whom I almost spent 2 years of my life in three different countries. Thank you to Emilie, Etienne and Quentin. This experience wouldn't have been the same without you.

TABLE OF CONTENTS

LIST OF FIGURES

LIST OF TABLES

CHAPTER 1: INTRODUCTION

In the past few decades, numerous studies have shown that flow has a significant impact on crystallization kinetics and morphology of semicrystalline polymers and therefore, on final properties [1]. Molecular characteristics such as molecular weight distribution, isotacticity, defects, etc. and imposed flow conditions, such as temperature, shear rate, etc. have a great influence of flow induced crystallization (FIC) [2] [3] [4] [5]. Processing of semicrystalline polymers, involves flow and thereby flow induced crystallization studies are important.

Theoretical and experimental work indicates that the final morphology is dictated by structures present in the melt at the early stages of shear and crystallization [6] [7] [8] [9] [10]. These structures are called *precursors* and their nature is currently under investigation [11] [12] [13] [14]. The purpose of this thesis is to study the relaxation process of shear-induced crystal nucleation precursors using a series of commercial isotactic polypropylene and random propylene-ethylene copolymers.

Many studies of FIC were dedicated to PP, PE, and also some on PB and PS but fewer have been done on random copolymers [13] [14] [15] [16]. Random copolymers are used in industry because of their improved impact resistance, flexibility and mechanical properties at low temperatures [17]. They are used in extrusion (film and sheet) and injection molding. So here, we examine the effect of comonomer on flow induced crystallization.

The thesis outline is defined as follows: the second chapter provides a theoretical and experimental background concerning flow induced crystallization and relaxation of shear-induced nucleation precursors. The third chapter contains the research methods including materials and experimental techniques used. In the fourth chapter, we describe and discuss our results on relaxation of crystal nucleation precursors. In chapter five, conclusions and perspectives are presented.

CHAPTER 2: BACKGROUND

2.1 Quiescent crystallization

Crystallization can occur when a polymer is cooled, below its equilibrium melting point, $T_{m,eq}$. In order to crystallize, the polymer melt which is composed of coiled and entangled molecules passes from one disordered state, to a partially ordered state in which there will be crystalline and amorphous regions. Therefore, polymers are always semicrystalline.

2.1.1 Nucleation and growth

Crystallization of a polymer under static conditions (in absence of flow) takes place in two steps [18]:

- Nucleation, is a phenomenon where appear the first crystal nuclei of a solid phase or a compound.
- Growth, where additional chain stems is deposited onto the nuclei and lamellae start growing from nuclei.

The theory of nucleation and growth for polymers is derived from the classical theory for small molecules [19]. The nucleation mentioned above corresponds to a homogeneous nucleation which does not involve a foreign matter but only the polymer melt itself. However, in practicality crystallization often starts by a heterogeneous nucleation, which requires the presence of a surface of a foreign matter which promotes the deposition of segments of macromolecular chains.

2.1.2 Morphology

Within the polymer melt, the macromolecular chains are organized in random coils. During crystallization, these coils are reorganized, partially, in lamellae with a thickness of the order of tens of nanometers, with some chain folding. These crystalline lamellae are alternately separated by amorphous regions which can contain some chains that connect them together (Figure 2.1).

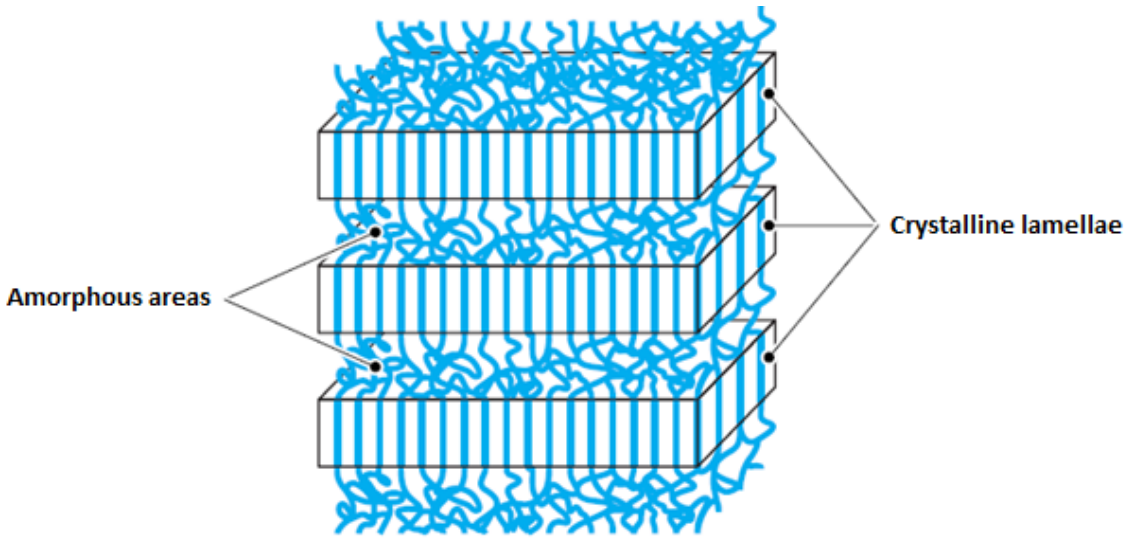

Figure 2.1: Crystalline lamellae and amorphous regions. ***Reproduced from reference*** **[20].**

Lamellae can arrange into different types of superstructures depending on the crystallization conditions and the specific nature of the polymer. For example, axialites consist a stack of crystallites growing in one direction. Axialite will close in on itself and grow to take a spherical symmetry shape [21].

Another type of arrangement called hedrite consists of polyhedral structures [22]. This arrangement is intermediate between single crystals (typically obtained through careful crystallization of a solution) and spherulites (obtained during crystallization from a melt).

Under quiescent conditions in the melt, lamellae are commonly organized into three dimensional superstructures called spherulites [23]. The growth direction (radial direction) of these spherulites always corresponds to a particular crystallographic direction.

Lamellae are oriented radially; therefore, within a spherulite, the main chain axis is oriented perpendicular to the surface of the lamellae and tangential to the spherulite. When observed by optical microscopy between crossed polarizer and analyzer, spherulites often show a cross-shaped extinction called “Maltese cross” along the axes of the polarizer and the analyzer (Figure 2.2). This phenomenon results from the dielectric nature of polymers, the nature of highly anisotropic crystals of polymers, and the organization of the crystals in the spherulite.

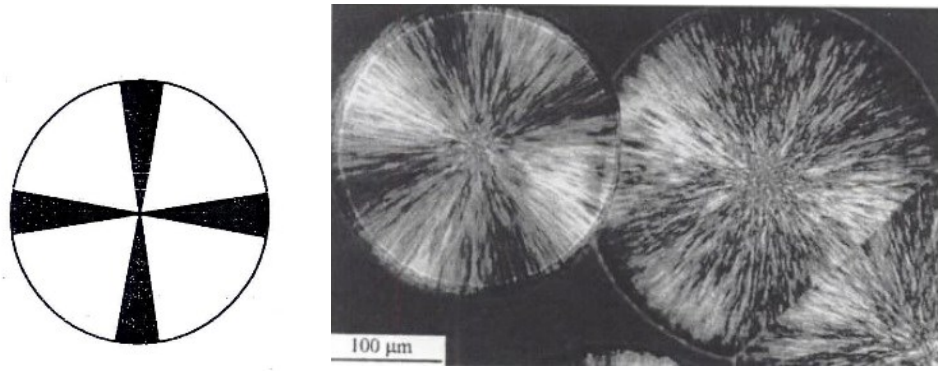

Figure 2.2: Left: cross-shaped extinction under crossed polarizers (Maltese cross), Right: Polypropylene spherulites observed by light microscopy between crossed polarizers. *Reproduced from reference* [23].

2.2 Polypropylene crystallization

During the polymerization of polypropylene, chain monomers can be incorporated in different configurations: head-to-tail, tail-to-tail and head-to-head (Figure 2.3). Due to steric hindrance, the methyl group (CH_3) promotes the head-to-tail chain configuration. In addition, the presence of asymmetric carbons leads to the formation of three possible

configurations which are distinguished by the distribution of hydrogen and methyl groups on either side of the plane formed by the carbon skeleton.

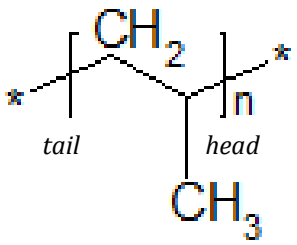

Figure 2.3: Polypropylene repeating unit.

If all methyl groups are located on the same side of the plane, the polymer is said to be isotactic (iPP, Figure 2.4 top). If the groups are alternately on either side of the plane of the carbon, the polymer is said to be syndiotactic (sPP, Figure 2.4 middle). Finally, if the distribution of groups is random, the polymer is said to be atactic (aPP, Figure 2.4 bottom). Isotactic and syndiotactic polypropylenes, which have a greater regularity of chains, are semicrystalline. However, the absence of steric periodicity prevents atactic polypropylene from crystallizing. At the present time, industry synthesizes and uses essentially isotactic polypropylene [24]. However, other polymer configurations are also technologically important. As an example, polystyrene (PS) has two known forms (syndiotactic and atactic), but atactic polystyrene is used most in industry [25].

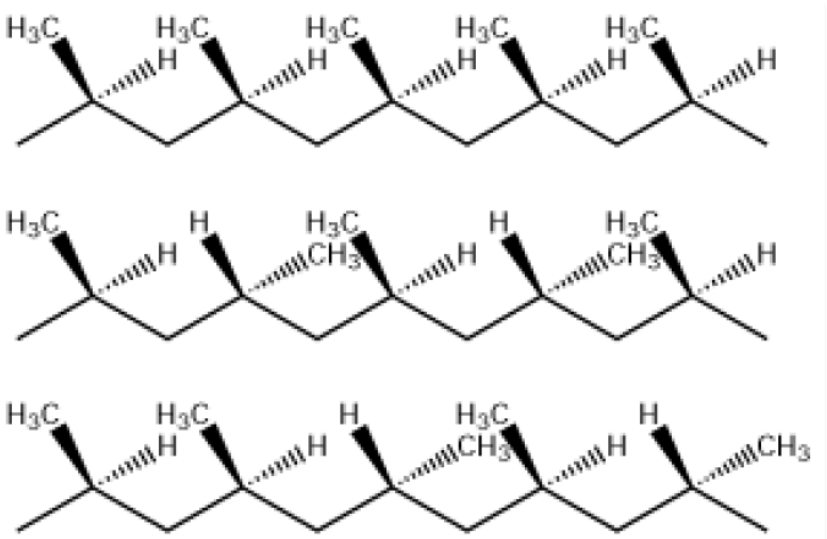

Figure 2.4: Top (isotactic PP), middle (syndiotactic PP), bottom (atactic PP).

Isotactic polypropylene chains are arranged helicoidally in the crystals [26]. Indeed, the helical structure is the most stable spatial conformation (minimum potential energy) of the chain [27]. iPP can crystallize into several different phases: monoclinic (α), hexagonal (β), triclinic (γ) and an intermediate structure called smectic.

The most common structure is called **monoclinic α** (Figure 2.5). It can be obtained by crystallization from the melt or from solutions. The cell unit dimensions are: $a = 6{,}65$ Å ; $b = 20{,}96$ Å ; $c = 6{,}50$ Å ; $\alpha=\gamma=90°$; $\beta = 99{,}33°$ and it has a density $\rho = 0{,}936\ g.cm^{-3}$ [26]. Its melting temperature is 165°C.

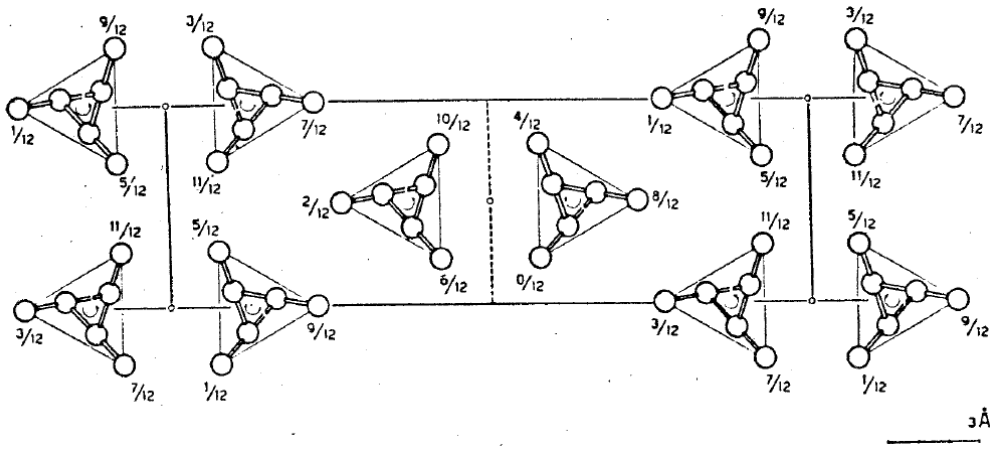

Figure 2.5: Crystalline structure of the α phase of iPP in the direction (001).
***Reproduced from reference* [8].**

The **hexagonal structure β** is metastable and can be obtained during crystallization from the melt. Keith and al. [28] were the first to reveal the existence of this phase. The growth rate of this β-phase is higher than that of the α phase in a crystallization temperature range between 100°C and 145°C, and its melting temperature is lower (145°C)

The **γ structure** is much less common and only appears from the melt with polypropylenes having a low molecular weight or under extreme pressure mass. [29]. The presence of defect also promotes the γ phase. Alamo and coworkers [30] found that materials possessing the same amount of defects but of different kind have identical γ phase contents at various crystallization temperatures. Its crystal structure has long been controversial and has only recently been elucidated [31]. The dimensions of the γ orthorhombic unit-cell are *a = 8.54 Å ; b = 9.93 Å ; c = 42.41 Å.*

Finally, the **smectic phase** of the polypropylene is generally formed at a low temperature of crystallization. This phase corresponds to molecules arranged in layers and can be obtained by quenching [32].

2.2.1 Random propylene / ethylene copolymers

Although polypropylene possesses very interesting properties, some limitations prompted the industry to develop copolymers [33]. Indeed, introduction of comonomers in the macromolecular chain leads to the creation of new morphologies and properties (thermal, optical and mechanical).

Copolymers can be categorized according to how the units are arranged throughout the chain. There are as follows: periodic, block and random copolymers. Periodic copolymers possess monomeric units that are distributed in alternating sequences. For block copolymers, sequences of monomeric units are followed by sequences of monomeric units of another type. Lastly, in random copolymers, the different types of monomeric units are randomly interspersed throughout the macromolecular chains.

It must be noted that in random copolymers, comonomer distribution may not be completely random. De Rosa [34] monitored the degree of segregation of defects in the polymer chains through the crystallization of α and γ phases. They found that in samples prepared with unbridged catalysts, the amount of γ form appears to be always lower than

for samples prepared with chiral isospecific catalyst. They concluded that defects in samples with unbridged catalysts are not randomly dispersed but more localized in certain areas of the chain.

Polypropylene random copolymers exhibit a decreased melting point. Presence of new monomer units has for effect to introduce irregularities within the polymer chain. This result an improved impact resistance, flexibility and mechanical properties at low temperatures, which is very important in domestic applications. They are used in extrusion (film and sheet) and injection molding. Food and medical packaging and consumer products are eager for this type of product.

Many studies have been carried out on the effect of the type of comonomer on the final physical properties. Besides ethylene is the most common comonomer used, other studies were dedicated to a fixed comonomer type such as pentene [35], alkene [36] octene [37], hexene [37] and butene [38]. Usually, polypropylene random copolymer contains between 1 and 7% weight of ethylene molecules and 99 to 93 % weight of propylene molecules [39].

Alamo and coworkers [5] studied the morphological distribution of ethylene defects in random propylene-ethylene copolymers using solid state NMR spectroscopy. They highlighted that 42% of the ethylene units, were included in the crystal for metallocene propylene/ethylene random copolymers with ethylene contents of 0.8-7.5% mol are

composed of. Presence of ethylene units as inclusions in the polypropylene crystal reduced the melting temperature of the copolymers. Therefore, these units act as defects in the polypropylene crystal (Figure 2.6). It should also be noted that the inclusion of comonomers in polypropylene crystals is not confined to ethylene molecules. De Rosa found that some butene (which is bulkier than ethylene) had been included in crystals of syndiotactic [40].

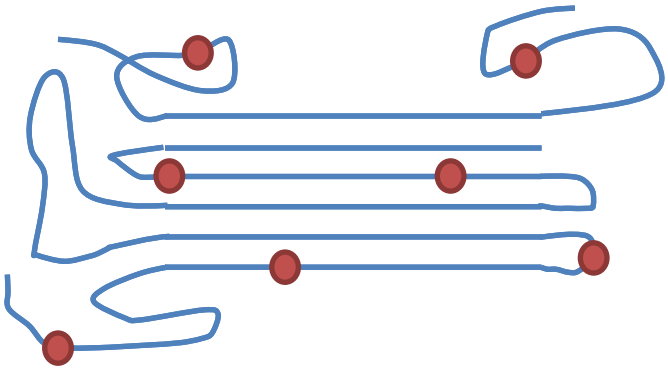

Figure 2.6: Inclusion of ethylene units in polypropylene chains

Other studies confirmed that inclusion of ethylene leads to decrease the crystallization and melting temperatures, and the overall crystallinity [41] . In addition, the increase of structural irregularities promotes formation of γ phase which has a large impact on the lamellar morphology [42].

2.3 Transcrystallization

Transcrystallization refers to the crystallization under quiescent conditions of a polymer in contact with a nucleating surface [43] [44]. Hence, it arises from a process of heterogeneous nucleation. Usually, fibers are used as the nucleating materials for transcrystallization studies, so the resultant morphology will be radial lamel1ar growth perpendicular to the surface (Figure 2.7 and Figure 2.8). These growing lamellae will be constrained laterally by other growing lamellae so oriented morphologies emerge. The rate of growth of the transcrystalline layer and of the spherulites in the bulk will be the same for fixed crystallization conditions.

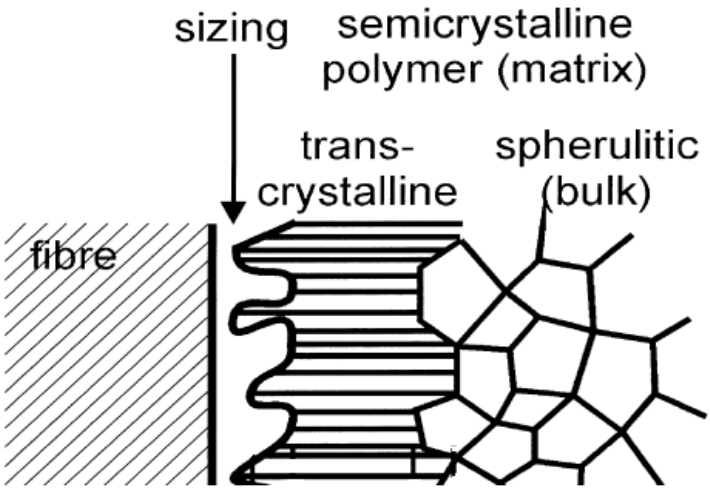

Figure 2.7: Transcrystallinity process. ***Reproduced from reference*** **[4].**

From an industrial point of view, when a piece is cooled, the cooling time will increase from the wall towards the middle of the piece and the resulting crystal structures will be affected. In the solid material, the spherulite size will depend on the number of nuclei

formed and thus on the degree of supercooling. Therefore, there will be smaller spherulites on the wall and larger towards the center of the piece [20].

In some cases, when the wall is not properly cooled, the supercooling and the cooling rate are low. There are few active nuclei and formed spherulites are large. The nuclei at the wall (often mostly dust) can cause the apparition of "*spherulites*" oriented perpendicular to the wall called transcrystallinity. The appearance of this layer can have implications for the performance of fiber-reinforced composites, so numerous researchers have studied it by changing the crystallization parameters or the type of polymer [45] [46].

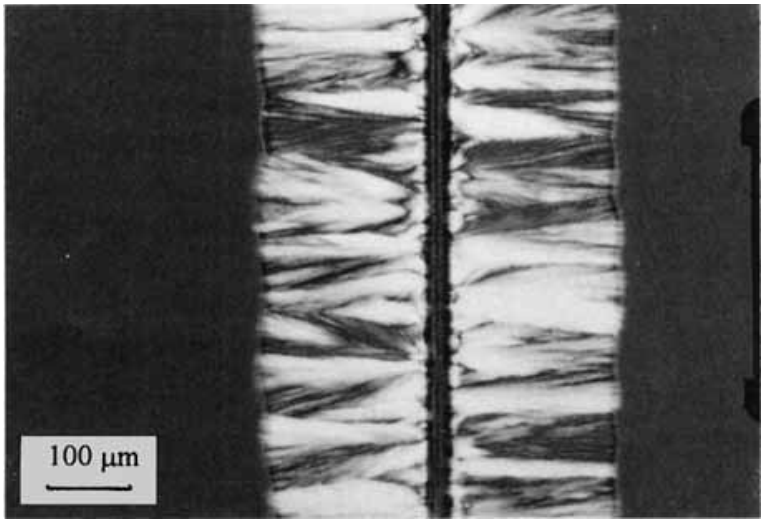

Figure 2.8: Transcrystallinity between a glass fiber and polypropylene matrix
***Reproduced from reference* [47]**

2.4 Flow-induced crystallization (FIC)

Flow induced crystallization (FIC) has a huge technological importance. In most polymer processing operations, the molten polymer is exposed to flow at different stages which affects the kinetics of crystallization and the morphology (such as "skin-core" effect, for example) of the product. Performance and properties (mechanical, optical, thermal, etc) are highly dependent on the specific structure of the final products, and therefore on FIC. In turn, the microstructure from FIC processes is strongly dependent on the molecular structure, temperature of crystallization, flow conditions and type of polymer used [48] [4] [49].

2.4.1 Models of flow-induced crystallization

For several years, application of a flow field onto a melted polymer has been known to promote crystallization. This phenomenon increases both the total number of activated nuclei (or nucleation points) and the nucleation rate [50], therefore increasing overall crystallization kinetics. Janeschitz-Kriegl showed that decreasing temperature and increasing mechanical work increases the number of nuclei by many decades [51].

In a quiescent melt, there is a huge reservoir of badly organized aggregates of chain molecules or called, "*dormant nuclei*", which can become effective nuclei under a flow treatment. These aggregates are supposed to be oriented in the flow direction. The action of flow will transform these dormant nuclei into better quality nuclei which can lead to

growth of precursors of shish-kebab structures [52]. These precursors present in the early stages of crystallization have been widely studied [53] [54] [55] [56], as they often dictate the resulting morphology and final properties of materials.

At the present time, two mechanisms have been proposed to explain the increase of the rate of crystallization. The first one considers that polymer molecules are entangled in a restricted molecular movement. As the stress in the melt increases, the chains become extended. A particular orientation will provide some lines of nucleation which can allow the growth of the lamellas. The second mechanism supposes that some heterogeneous particles in the melted polymer can create localized flow disturbances. The quantity of stretched molecules will then increases and enhance nucleation along the fiber [47].

In early studies, Mackley and Keller [57] highlighted that alignment and stretching of polymer chains by flow reduces entropy and modifies free energy, necessary for the apparition of crystallization. However, this is not enough to explain the increase in rate of crystallization. Similarly, it has been highlighted that if the polymer chains are extended, the “kinetic barrier” which must be overcome for crystallization to occur will be reduced. Indeed, this state of this extended polymer is not far from the state of a final crystal as compared to a random coil [58].

2.4.2 Flow-induced crystallization morphology

The oriented morphology typical of FIC is called shish-kebab in which lamellar crystals grow outward from an aligned cylindrical core (Figure 2.9) [59]. It was found by Keller, for crystallization of polymers in solution with elongational flow [58] [60].

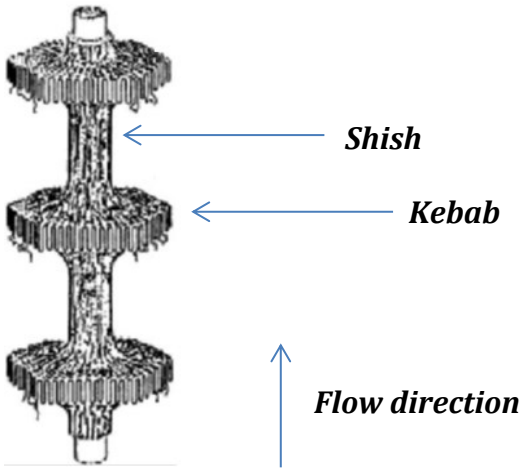

Figure 2.9: Illustration of a shish-kebab crystal structure. ***Reproduced from reference*** **[48].**

Shish-kebabs consist of a central fibrillar area ("shish") and radially growing lamellae ("kebabs"). They result of a two-step process: first, the "shish," possessing extended or partially extended chains, is formed parallel to the direction of flow. Then, the crystalline lamellae grow epitaxially on the "shish" previously created [61]. Nevertheless, the exact mechanism of shish formation is still a subject of debate.

Also found in melts, some studies performed with Transmission Electron Microscopy (TEM) highlighted the presence of "shish-kebab" structure out on samples of isotactic polypropylene crystallized after shearing [61] [62]. The crystalline lamellae that grow from the "shish" are parallel, and their distance is estimated about 10 to a few tens of nanometers [48].

In his research on polymer processing of polyethylene blown films, Haudin [63] indexed changes in morphologies of a polymer depending on the intensity of the flow. One can then pass from a spherulitic morphology, to flattened spherulite, then to sheaf-like texture and finally to the cylindrites models of Keller (shish-kebabs) (Figure 2.10).

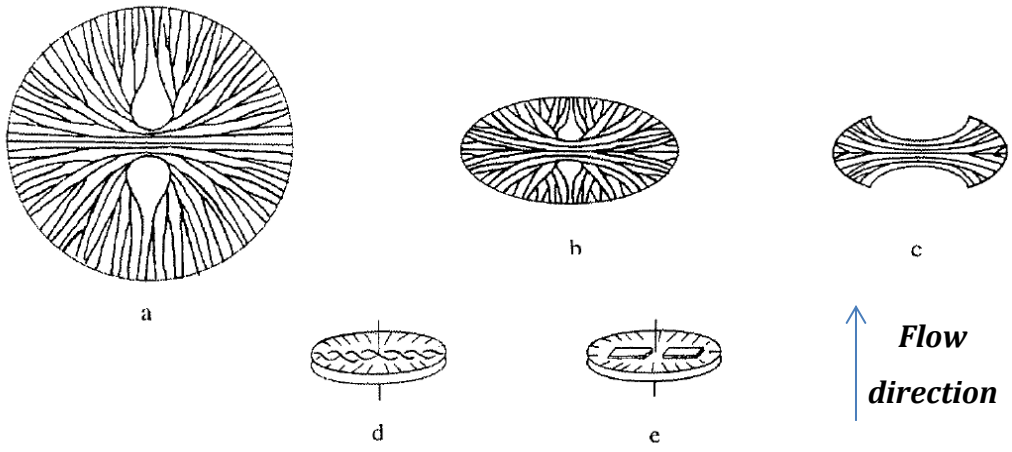

Figure 2.10: Morphologies evolution depending in the intensity of flow a) Spherulite b) Flattened spherulite c) Sheaf-like morphology d) and e) cylindrites models of Keller. ***Reproduced from reference*** **[63].**

The phenomenon of "row nucleation" which has been known for nearly forty years must be mentioned [64]. It consists of an alignment of morphologies (lines of nuclei with aligned molecules) along the direction of flow [65] and has been observed on isotactic polypropylene (iPP) [66], on polyphenylene sulfide (PPS) [67] and in polystyrene [65]. Varga and Karger [68] have shown the presence row-nucleated cylindritic crystallization in glass fiber-reinforced polypropylene composites and demonstrated that the crystalline form of polypropylene (α, β, γ) can be produced preferentially under given crystallization conditions.

Mackley [69] showed that some shear rate need to be reached to start shish kebab growth process, chain extension and orientation. Finally, the effect of the deformation caused by extensional flow has been investigated for isotactic poly-1-butene [70]. A major effect was the enhancement of the thread-like precursors which we know are required for the formation of shish-kebabs crystal structure. SAXS (Small Angle X-ray Scattering) revealed an increase in crystallinity, due to the increased orientation the polymer.

A innovative technique called "short term shearing" has been developed to study flow induced crystallization at high shear rates [53] [71]. This method involves application of a flow for a time short enough to obtain nucleation derived from the initial brief pulse of shear and a temperature high enough to get slow growing crystal. Results have led to a phenomenological model [54] [71] [72]. A formation of point like nuclei will grow up

into threadlike precursors during shear, resulting in a radially crystals growing outwards from these nuclei.

Injection molded samples can possess different crystalline areas: close to the wall, where the shear rate is the strongest, oriented structures will appear. In the center, there will be isotropic spherulites, due to lower stresses. Finally, in the middle, a “fine-grained” layer can be observed (Figure 2.11). According to Jerschow and Janeschitz-Kriegl, this layer consists of anisotropic oblong crystals aligned transverse to the flow [54].

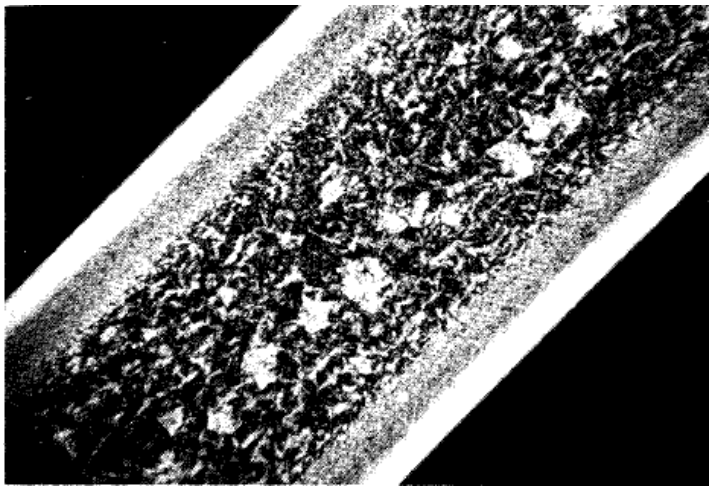

Figure 2.11: Cross section of iPP after short term shearing. ***Reproduced from reference*** **[27].**

Other studies have been interested in the formation of precursors [11] [73] [74] [75] [9]. Several evidences of the existence of these metastable structures have been reported with in situ techniques (X-ray scattering) as well as ex situ techniques (optical and electron microscopy).

Rheo-SAXS in sheared polypropylene melts showed structures of row-nuclei onto which lamellae can develop [12]. A shear impulse close to the thermodynamic melting temperature created a metastable suspension of shishes in HDPE observed by SAXS and WAXD [7]. Rheo-optical techniques with duct flow showed a change in the birefringence during flow [11] [8]. By optical microscopy and X-ray scattering, a formation of micrometer structures in isotactic polystyrene sheared above the melting temperature was found [76]. These studies have demonstrated that precursors are formed in the very early stage during the crystallization process after the shear.

2.4.3 Effect of processing conditions on FIC

In processing conditions, when a polymer is subjected to high shear flow rates, a critical shear rate and shear strain are needed to create strongly oriented shish-kebab structures [77]. Kumaraswamy and al. [73] showed that application of a short pulse of shear in iPP reduced crystallization time by two orders of magnitude. Increasing this shearing time led to a saturation of the crystallization time and anisotropic structures have been observed. According to the authors, these structures can be linked to the formation of a “skin core” morphology already described by Eder and Janeschitz-Kriegl. An increase in temperature

can lead to a decrease of the time of formation of the precursors. Some studies investigated the influence of shear rate and duration of shear on crystallization kinetics. The increase in each of these two parameters generally leads to a faster overall kinetics [55] [54].

Even though overall kinetics of crystallization is increased with flow, it must be define to be due to an effect of nucleation, growth or both to determine if these parameters has an influence on the crystallization. Most of the available literature converges in the same direction, showing an increase in the number of nuclei in the polymer supercooled. [18]. On the other hand, the influence of shear on the growth rate has been less studied and from an experimental perspective, these data are difficult to obtain [50] [78]. However, one group has reported a significant increase in the growth rate compared to the quiescent condition for fiber pulling experiment [4].

Tribout [50] has studied the behavior of nuclei as a function of crystallization temperature. He pointed out that the number of nuclei increases significantly when shear is applied, and especially as the shear rate increases. However, he noted an apparent saturation from a shear rate limit.

2.4.4 Effect of molecular attributes on FIC

Experimental studies have been performed to confirm the sensitivity of the crystallization (under or after shear) even with very low differences in molecular structure. It has been shown that the addition of a small proportion of long chains in the polymer leads to the formation of a shish-kebab structure [79].

Vleeshouwars [80] performed experiments on isotactic polypropylene with different molecular weight and molecular weight distribution (narrow, medium and wide) and a fixed shear rate. They found that improvement of crystallization was better with the high molecular weight samples. Jay [2] also observed that the sensitivity of a given polypropylene to shear depends on its molecular weight. They confirmed the hypothesis of Vleeshouwars [80]: the higher the molecular weight, the more enhanced the nucleation and then the crystalline growth rate. More recently, Small Angle X-Ray Scattering (SAXS) was performed by Somani and Al [10] for isotactic polypropylene after an isothermal shear flow step. The authors suggested that polymer molecules above a "critical orientation molecular weight" (M*) could give oriented structures at a given shear rate ($\dot{\gamma}$).

Bove and Nobile [81] [1] studied structural changes in the passage from the melt to the solid by measuring the storage modulus, which increases during the process of crystallization. Crystallization kinetics were strongly enhanced with the application of a shear flow on the poly (1-butene) samples with a different molecular weight but a similar

molecular weight distribution (MWD). Baert [3] found that poly (1-butene) with the highest molecular weight is most sensitive to shear flow. Rheological and structural investigations have interested researchers [82] and a critical value of shear rate $\dot{\gamma}_c$ was determined.

Influence of co-monomer content on flow induced crystallization has been investigated. For propylene-ethylene random copolymers, ethylene units lower melting and crystallization temperatures compared to iPP. Housmans showed that the effect of flow on crystallization kinetics decreases with increasing ethylene content [17].

2.4.5 Lifetime of precursors

The lifetime of FIC precursors is being investigated by several groups [14] [13] [83] [6]. The main physical phenomenon governing the disappearance of these precursors is named “melt memory”. If a semicrystalline polymer is heated up above its nominal melting point and then cooled down, some crystals will remain and the crystallization kinetic will be improved. The residual crystallites in the molten polymer can be erased if the polymer is held during a certain annealing time at high enough temperature. Flow induced crystallization studies have shown that, even at high temperature, the residual oriented structures created during flow can persist for very long times [14].

Alfonso’s group has been interested in the relaxation process of shear-induced crystal nucleation precursors in isotactic poly(1-butene)s with different molecular weights [14].

The indicative parameter in such experiments is the full disappearance of the oriented cylindritic morphology along the fiber (Figure 2.12). Several relaxation temperatures were used to find critical relaxation times, which were fitted with an Arrhenius plot. It was confirmed that the flow induced precursors disappear faster as the temperature increases. Systems with short chains are able to relax much faster than those containing fraction of high molecular weight chains. Apparent activation energies are independent of the length of the constituent chains [14]. An Arrhenius plot which displays the logarithm of kinetic constants plotted against the inverse of temperature will gives a straight line, from which the activation energy can be deduced and is widely used [14] [8] [15] [16] [84] (Figure 2.13). Others techniques can be used: Janeschitz-Kriegl and Isayev used duct flow and different range of relaxation temperature [8] while Cavallo used a rotational device [16].

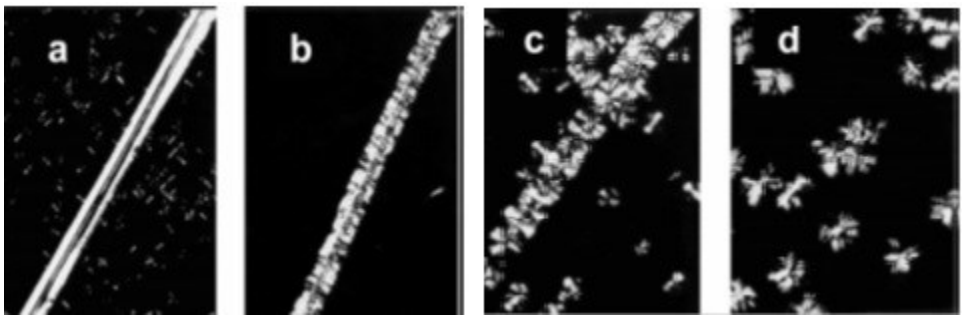

Figure 2.12: Morphological evolution in i-PBu 0200.
All samples were sheared and relaxed at 132.5 °C and isothermally crystallized at 90 °C.
(a) t_R 6 s, (b) t_R 60 s c) t_R 420 s, (d) t_R 690 s. Reproduced from reference [57].

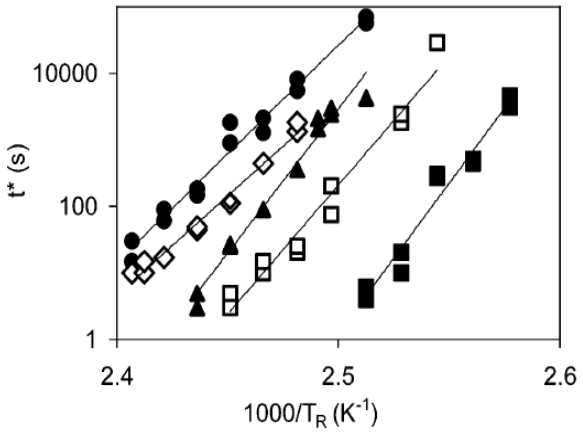

Figure 2.13: Critical annealing time required for disappearance of shear induced nucleation precursors as a function of reciprocal annealing temperature and various molecular weights. Mw = 850 000 (●), Mw = 398 000 (◊), Mw = 295 000 (▲), Mw = 177 000 (□), Mw = 116 000 (■). *Reproduced from reference* [57].

2.4.6 Types of FIC experiments

Industrial processing operations involve complex flow and thermal histories, prior to and during the phase transition. Individual studies attempt to provide an understanding of the intrinsic nature of these phenomena by using experimental techniques in which flow and temperature are more precisely controlled.

2.4.6.1 Couette flow

One of the first polymer crystallization studies were performed using Couette type viscometers. Kobayashi and Nagasawa [85] observed a rapid increase of the rate of crystallization when polyethylene was sheared. Electron micrographs of the surface showed lamellar crystals growing perpendicular to the flow direction. Somani and al [86]

combined Small-Angle X-ray Scattering (SAXS) and Wide-Angle X-ray Diffraction (WAXD) and Couette flow geometry to investigate thermal stability of shear-induced oriented precursor structure in isotactic polypropylene. They obtained the first quantitative measures of the limiting temperature at which no oriented structures survive.

Cylindrical rheometers have some drawbacks, in particular the presence of temperature gradients within the melt, due to the viscous heating effects. The large size of the machine makes it difficult to control the crystallization temperature and the cooling of the melted polymer. To avoid these problems, parallel plate devices have been developed.

2.4.6.2 Sliding plates

Establishment of shear flow can be obtained by the simple motion of one flat plate relative to another. A frequently used technique is to place a thin film of polymer between two glass slides and apply a translation on one of the glass slide, thereby creating a shear stress. Studies have been done by Lagasse and Maxwell [49] to investigate the effects of shear on induction time. With low molecular weight polyethylene they observed that there is a critical shear rate above which shear flow begins to accelerate crystallization.

2.4.6.3 Capillary flow

In melt processing, during injection or extrusion, pressure is often used to drive flow through tubes. Thus, in order to represent the process of injection molding more accurately, capillary experiments can be performed. Titomanlio and Marrucci [87] used a modified capillary device under pressure to carry flow induced crystallization on High-density Polyethylene (HDPE). Results showed that the crystallization temperature is influenced by the shear flow along the capillary and at the entrance of the capillary.

2.4.6.4 Rheometers

Rheometers are the most commonly used device for shearing molten polymers [16] [88]. Studies of shear induced crystallization used directly rheometer with plane-plane geometry or cone-plate. However, in most cases, rheometers are modified or equivalent devices are built. Also, shearing cells with parallel plates with rotational flow [49] [78] [89] have been specifically designed for the study of the crystallization of molten polymers.

Experimental difficulties associated with the study of flow induced crystallization in rheometers are numerous. The point is controlling thermal and mechanical conditions, allow measurements and ideally achieve in situ observations.

2.4.6.5 Fiber pull-out

Fiber pull-out provides a shear flow which is created by the axial movement of a fiber embedded within a polymer matrix placed between two glass slides [90] [14]. In most cases, a polarized optical microscope is used to monitor morphology development during crystallization. In most cases, crystalline structures in the vicinity of the fiber are similar to those obtained during transcrystallinity experiments. However, for shear experiments, the fibers must have been chosen because of their non-nucleating power towards to the polymer. The highly oriented structure originates from a prolific nucleation around the fiber induced by flow. Research has shown that the nature of the crystalline phase obtained depends on thermo-mechanical conditions [14]. Figure 2.14 shows the cylindrical crystallization of poly-1-butene induced by traction of a glass fiber at a temperature of 122.5°C. Under certain shear temperatures or crystallization temperatures, the growth of the α phase may continue in β phase [91].

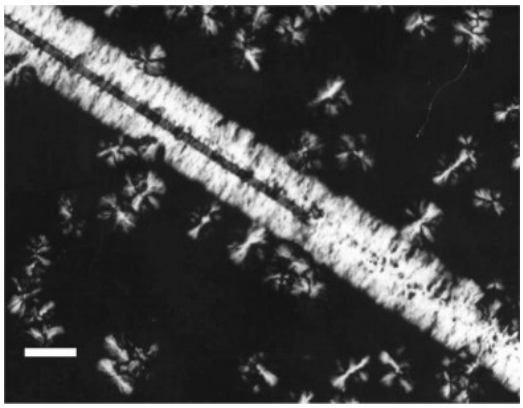

Figure 2.14: Cylindritic morphology around a pulled glass-fiber, at T_{pull} = 122.5°C and with an isothermal crystallization at T_c = 90°C. The white bar corresponds to 100 μm.
Reproduced from reference **[57].**

CHAPTER 3: RESEARCH METHODS

3.1 Materials

3.1.1 Polypropylene and random propylene-ethylene copolymers

We used an isotactic polypropylene homopolymer produced by Borealis, grade HD234CF and two propylene/ethylene random copolymers, grades RD204CF and RD208CF, respectively. Their characteristics are shown in Table 3.1.

In this study, the homopolymer is denoted as "iPP" while the copolymers are denoted as "RACO3" and "RACO7", according to their respective ethylene content in mol % (Figure 3.1). All three materials are commercial resins and were synthesized by bulk polymerization of propylene in the gas phase using a Ziegler-Natta catalyst. The nominal melting temperatures are 164, 153 and 139°C for iPP, RACO3 and RACO7, respectively [92] [17].

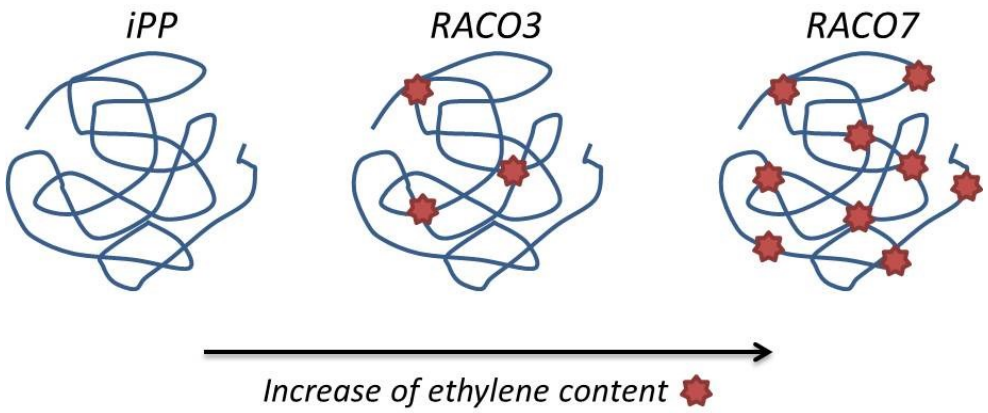

Figure 3.1: Schematic of molecular structure of iPP, RACO3 and RACO7.

Table 3.1: Molecular and physical properties of iPP and copolymers.

[a]Measured by NMR [b]Measurements were performed under a heating and cooling rate of 10 °C/min.

Reproduced from reference **[17]**.

Polymer	*Grade*	*Ethylene content (mol %)*[a]	X_c *(%)*	T_m *(°C)* [b]	T_c (°C) [b]	M_n *(kg.mol^{-1})*	M_w *(kg.mol^{-1})*	DPI
iPP	HD234CF	0	49.5	164	110	91	310	3.4
RACO3	RD204CF	3.4	41.3	153	105	91	310	3.4
RACO7	RD208CF	7.3	33.9	139	98	91	310	3.4

All three grades possess a melt flow rate of 8 g/10 min, a weight-average molecular weight (M_w) of 310 kg.mol^{-1} and a polydispersity index ($DPI = \frac{M_w}{Mn}$) of 3.4. Molecular weight averages were determined by Borealis with a high-temperature size exclusion chromatography (135°C) using trichlorobenzene as a solvent [92].

3.1.2 Fibers

We considered three types of glass fibers for application of the fiber pull-out technique (Table 3.2). Glass fibers with polypropylene sizing were excluded as the effect of the coating could not be separated from the effect of the type of PP matrix used.

Table 3.2: Fibers properties

Grade	Sizing	Diameter *(μm)*	Filaments per strand	Linear density	
				Yds/lb	*Tex*
#FGI Flexstrand 110EM13347 FiberGlass Industries	0,5% wt organic 98% wt LMW epoxy.	16	2000	450	1100
FiberGlass Industries	96% wt Cationic Maleated HMW PP 2% wt Nonionic Maleated PP 2% wt nonionic Paraffin wax	-	-	-	-
#EC13 272 Z20 T6M H9 Vetrotex	Starch/silane binder	13	800	1.8	272

Glass fiber sizing is generally a proprietary mixture of several compounds chemically bonded to the fiber that promote compatibility between the fiber and a resin matrix. Other processing treatments such as lubricants, film formers, wetting agents, crosslinking agents and antistatic agents can be used to improve the overall performance of the fiber [93]. Fiber *#FGI Flexstrand 110EM13347* from FiberGlassIndustries was used for most

experiments. It is designated to be most compatible with polyester, vinyl ester, epoxy, phenolic and urethane resin systems. Few experiments were performed with fiber *#EC13 272 Z20 T6M H9* from Vetrotex. It was checked that neither fiber #FGI Flexstrand110EM13347 from FiberGlassIndustries and fiber #EC13 272 Z20 T6M H9 from Vetrotex should not induce transcrystallinity under quiescent conditions (when not pulling is applied).

Dimensions of the Fiber *#FGI Flexstrand 110EM13347* were verified with an Olympus BX51 Polarized Optical microscope (Figure 3.2). An average diameter of 16.90 μm was found.

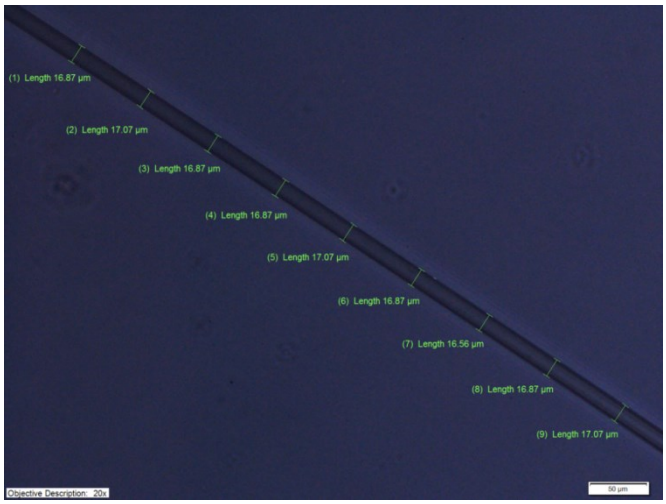

Figure 3.2: Diameter measurements along the fiber #FGI Flexstrand 110EM13347 with optical microscopy.

In addition, fibers were found to have a smooth surface, without impurities or particles by Scanning Electron Microscopy (Figure 3.3).

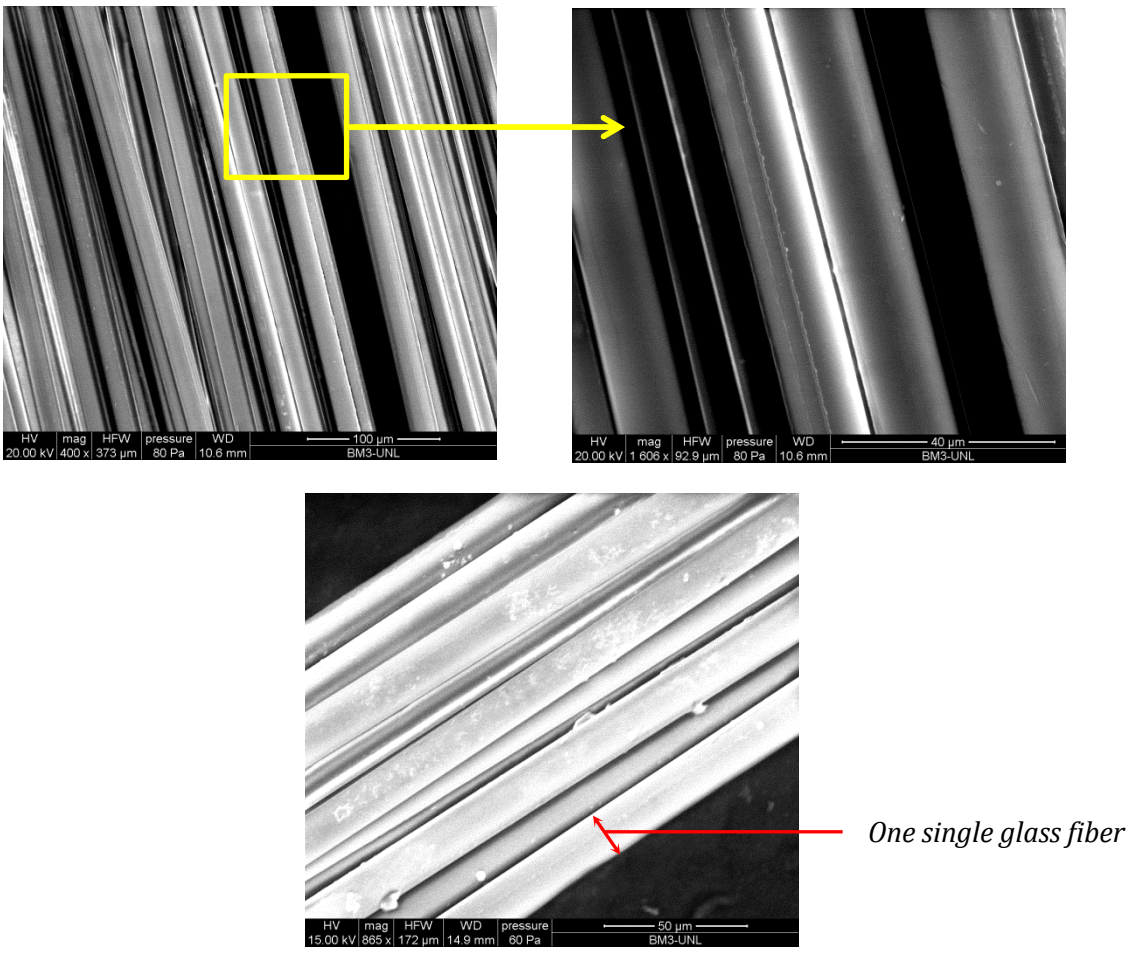

Figure 3.3: Scanning electron microscopy images of the glass fiber #FGI Flexstrand 110EM13347.

3.2 Experimental techniques

3.2.1 Sample preparation

Polypropylene films were first compressed molded with a manual 15-ton Specac hydraulic press. Fifteen or thirty PP pellets are sandwiched between two thin aluminum sheets within a 0.250 or 0.500 mm thick washer (Figure 3.4). This assembly was placed between two 75x75 mm² metal plates and heated to 215°C. After one minute, a pressure of 1 ton (13.8 psi) was applied for another one minute. Then, the melt was air-cooled. Final thickness of the films obtained was 250 and 500 µm.

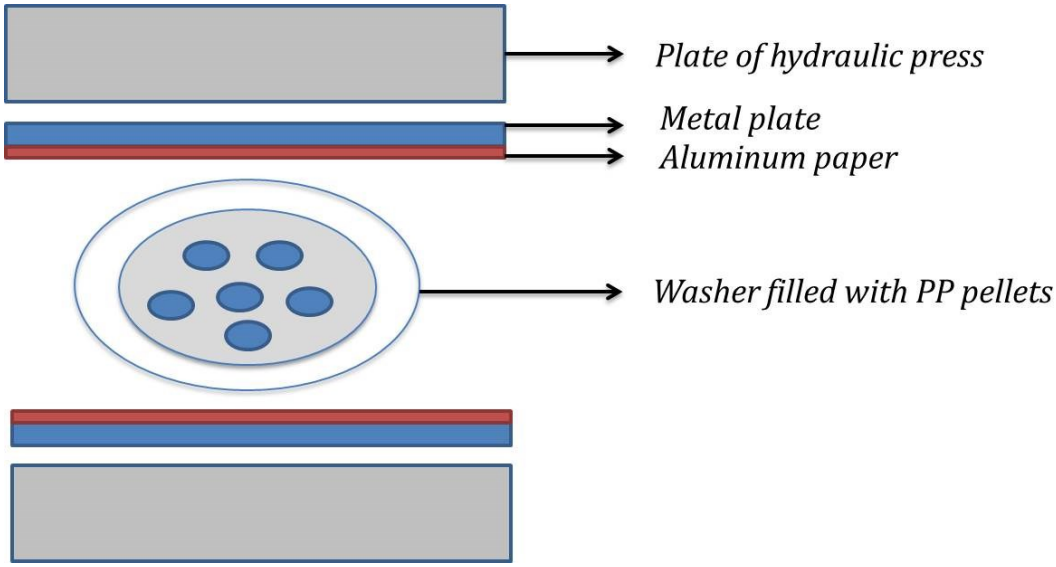

Figure 3.4: Schematic of sample preparation with hydraulic press

10x5x0.5 mm^3 samples were cut from the compression-molded films. Uniformity of the samples was verified by measuring thickness in several positions including the central areas. Each microscope slide and cover slide were cleaned with ethanol to eliminate any dust particles.

The microscope slide and cover slide dimensions were 25x75x1mm and 24x50x1mm, respectively. An individual elementary fiber was extracted from the bundle of fiber, which contain approximately 2000 fibers. Care was taken to extract only fibers in the middle of the beam, so that there is no bending along the fiber.

To prepare the composite, one glass fiber was placed between two polypropylene films (Figure 3.5). This set was subsequently sandwiched between one glass slide and one cover glass and placed in a Mettler Toledo FP90 (Thermo System) coupled with a FP82HT hot stage.

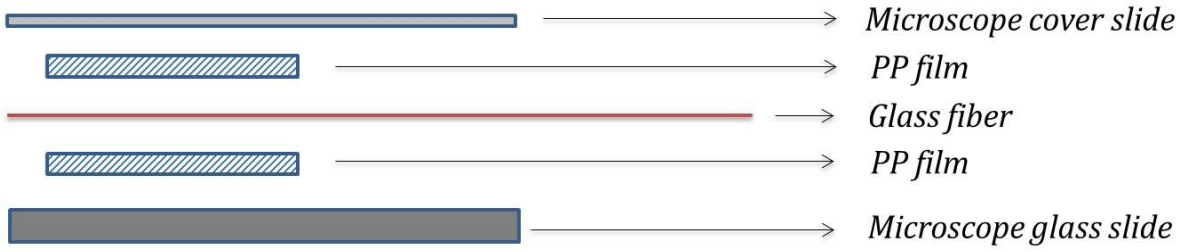

Figure 3.5: Schematic showing the sample composite layers

3.2.2 Thermomechanical history

In the hot stage, the ensemble was subjected to one or two different thermomechanical history procedures (Figure 3.6 and Figure 3.7). First, the as-prepared samples were heated to T_{erase} = 215°C for t_{erase} = 5 min, to erase the previous thermal history of the polymer. T_{erase}, is close to equilibrium melting point of iPP ($T_{m,eq}$ = 208°C) but no significant degradation is expected to occur [94]. As soon as at $T_{erase,}$ a slight pressure was applied to ensure that the fiber is well embedded within the polymer and to avoid any air bubbles.

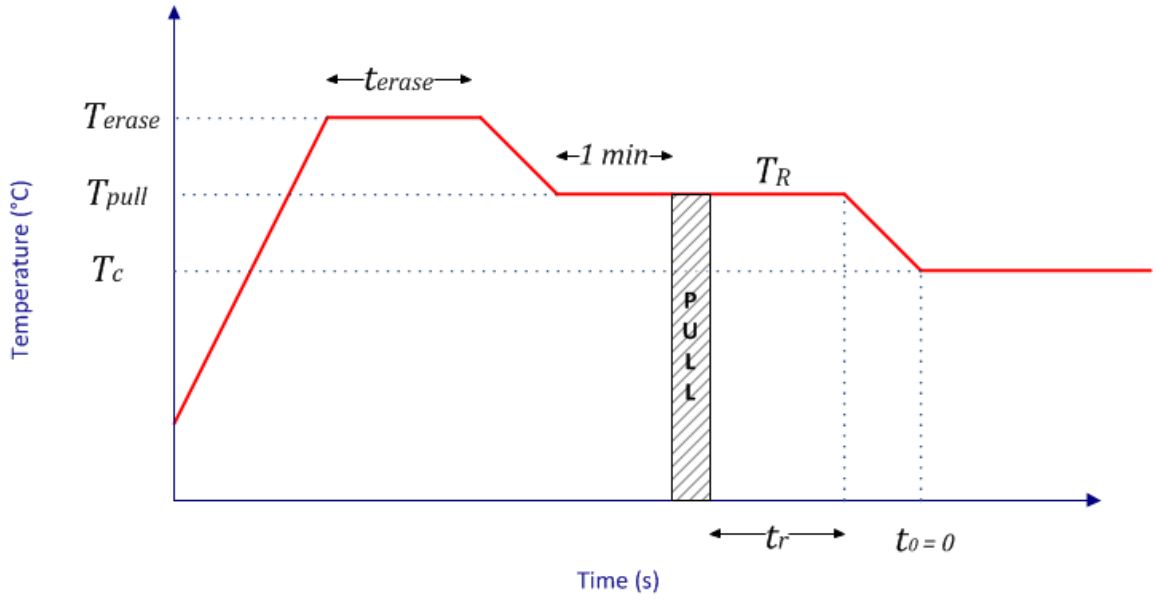

Figure 3.6: Thermomechanical history with $T_{pull} = T_R$ (procedure 1)

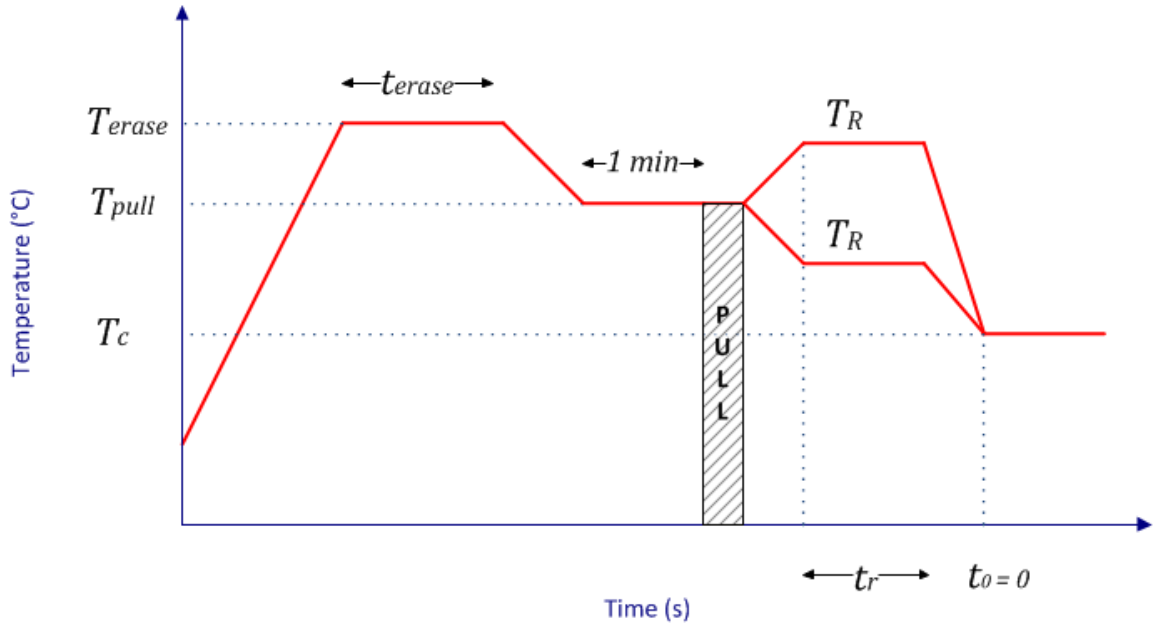

Figure 3.7: Thermomechanical history with T_{pull} = constant and $T_{pull} \neq T_R$ (procedure 2)

Then, the temperature is lowered at 20°.min^{-1} to a suitable pulling temperature, T_{pull}, which was always above the nominal melting temperature. Typically temperatures of pulling are reported in Table 3.3. The sample was kept at T_{pull} for one minute to allow for temperature equilibration. The fiber was pulled manually through the molten polymer at a linear velocity in the range of 5-10 mm.s^{-1} over a distance of 5-10 mm. Alfonso's group [14] found that fiber pulling experiments are nearly insensitive to both the extent of fiber

displacement and the rate of pulling. Indeed, experiments in which the fiber was manually pulled by different operators showed results differing less than 10% from those obtained by an automatic device.

Table 3.3: Temperatures of pulling.

Polymer	Pulling temperature $T_{pull} = T_R$ (°C)	Pulling temperature $T_{pull} \neq T_R$ (°C)
iPP	168.5-185	174
RACO3	170-182	170
RACO7	160-175	162.5

After pulling, the sample was allowed to relax at a given temperature T_R for a specified relaxation time, t_R. The relaxation temperature, T_R, could be equal (Figure 3.6 procedure 1) or different (Figure 3.7 procedure 2) than T_{pull} but was always higher than the nominal melting temperature. In the procedure 2, heating and cooling were done at 20°C.min^{-1}.

After the relaxation time t_R had elapsed, the sample was cooled down at 20°C.min^{-1} to its final crystallization temperature T_c. The final crystallization temperatures were chosen such that crystallization could be clearly observed on the order of minutes with relatively low nucleation densities throughout the bulk of the sample (Table 3.4).

Table 3.4: Crystallization temperatures.

Polymer	Crystallization temperature (°C)
iPP	135-138
RACO3	128
RACO7	120-122

The reference time, noted as t_0, was measured when T_c was reached. At the end of the experiment, the assembly was removed from the hot stage and air-cooled. The composite was then removed from the slides and its final thickness was measured.

3.3 Experimental devices

3.3.1 Mettler Toledo Hot Stage

A Mettler Toledo FP900 Thermo System, coupled with a FP82HT hot stage was used. The accuracy of the hot stage from 100 to 200°C is ± 0.6°C. The temperature in the hot stage was calibrated using benzoic acid (T_m=122.41°C) as a standard. The rate of heating or cooling was controlled to ensure that the programmed heating and cooling rates of 20°C.min^{-1} were attained by the hot stage in the range of temperatures used.

The FP82HT hot stage was placed in a polarizing optical microscope under transmission conditions.

3.3.2 Polarized Optical Microscope

A polarizing optical microscope Olympus BX51 equipped with a DP73 digital camera and an objective of 20x magnification was used. The microscope is equipped with a polarizer, positioned in the light path before the sample, and an analyzer (a second polarizer), and placed perpendicularly to the polarizer right after the sample.

Microscopic observation of flow induced crystallization was performed by placing the fiber at 45 degrees, with respect to polarizer and analyzer (Figure 3.2), in order to maximize the visualization of the oriented birefringence structure. Images were also obtained by introducing a quarter wavelength retardation plate after the sample and before the analyzer. This was done to ensure that growth of weakly birefringent regions was accurately observed. This accessory introduces a phase shift of 90 degrees between the ordinary and extraordinary axes when the plate is illuminated with linearly polarized light.

Images were recorded with a 1600 x 1200 resolution using the Olympus Stream Micro-Imaging Software. Exposure times were adjusted manually to optimize contrast and ranged from 30 to 200 ms.

3.3.3 Scanning Electron Microscopy

Characterization of glass fibers were performed with a Quanta 200 FEG Environmental Scanning Electron Microscope (ESEM). Images were taken at a high vacuum, with an electron beam voltage of 20 kV and a chamber pressure of 80 Pa.

3.3.4 Flow parameters of fiber pulling experiments

The axial movement of a fiber in a molten polymer will impose the shear rate $\dot{\gamma}$, with a cylindrical geometry (Figure 3.8):

$$\dot{\gamma} = \frac{dV_z}{dr} \tag{1}$$

where V_z is the component of the polymer velocity in the direction of the fiber axis (i.e. the z-axis in cylindrical coordinates) and r is the radial coordinate.

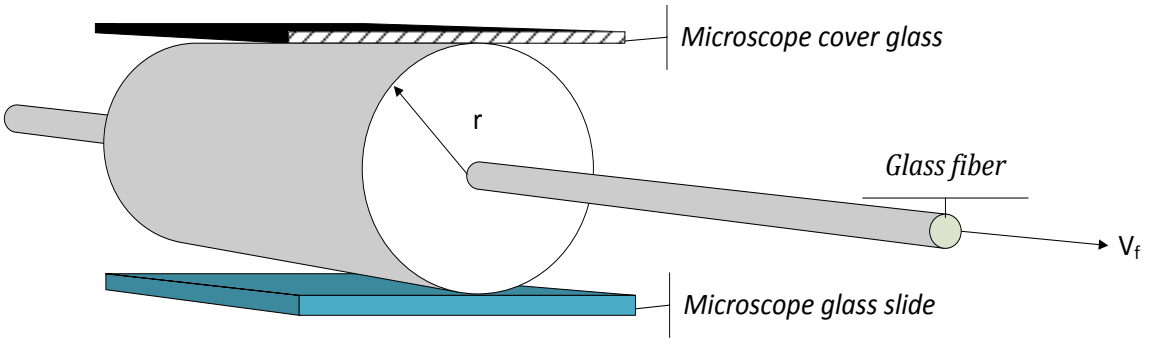

Figure 3.8: Geometrical movement of the embedded fiber.

A power law is assumed to describe the viscosity of the polymer

$$\boldsymbol{\eta = m(T)\dot{\gamma}^{n-1}} \tag{2}$$

where m(T) is a temperature dependent proportionality constant. The shear rate can be deduced from the force balance equation:

$$\boldsymbol{\frac{\eta}{r}\frac{\partial V_z}{\partial r} + \frac{\partial \eta}{\partial r}\frac{\partial V_z}{\partial r} + \eta\frac{\partial^2 V_z}{\partial r} = 0} \tag{3}$$

With the viscosity power law, the equation can be reduced to:

$$\boldsymbol{\frac{\partial \dot{\gamma}}{\dot{\gamma}} = -\frac{\partial r}{r}} \tag{4}$$

Our boundary conditions are: at the fiber surface, noted r_f, the velocity V_f is assumed to be the same as the fiber velocity, assuming no slip. At a radial distance far away from the fiber, noted r_e, the velocity is almost zero. Making the integration of this equation with the following boundary ($V_z = V_f$ for $r = r_f$ and $V_z = 0$ for $r = r_e$) leads to:

$$\boldsymbol{\dot{\gamma} = \frac{1-n}{n}\frac{1}{r^{1/n}}\left[\frac{1}{r_f^{1-1/n} - r_e^{1-1/n}}\right]V_f} \tag{5}$$

where n is the exponent in the viscosity power law equation. This equation is the same as shown by Monasse [90].

CHAPTER 4: RESULTS AND DISCUSSION

The type of morphology that develops in quiescent conditions after having pulled a fiber through a polymer melt is a highly sensitive marker of any residual molecular perturbation in the molten polymer.

Many research groups have focused on the study of flow induced nucleation precursors, using many techniques: rheo-optical [14] [13] [15], X-Ray scattering [16] [7] [12], FTIR spectroscopy [95].Although several attempts have been made to probe the precursor's morphology and relaxation (such as X-ray scattering, rheo-optical techniques or optical microscopy), mechanisms governing their disappearance involve more than a simple recovery of the polymer chains. Moreover, decay of flow memory is affected by structural and morphological features of the precursors [16].

Despite its simplicity, fiber pulling in a molten polymer is one of the best approaches in terms of sensitivity since nucleation density and growth morphology are affected by shear flow. Kinetic values of relaxation processes such as apparent activation energies may lead to a more thorough understanding of relaxation process of precursors.

4.1 Choosing experimental parameters

Calculations were performed to choose adequate experimental parameters: velocity of fiber pulling and film thickness. The obtained results were compared to the parameters used previously in the literature.

Equation (5) from section 3.3.4 [90] was first used to determine a minimum value of film thickness. The shear rate $\dot{\gamma}$ versus the distance from the fiber axis r was calculated for several film thicknesses, and the maximum value of shear rate $\dot{\gamma_{max}}$ in the melt (i.e. at the fiber surface) was determined (Figure 4.1). The exponent of the rheological power law of n = 0.2937 was taken for typical industrial polypropylenes [47]. The fiber diameter (measured previously in section 3.1.2) was 8.45 µm. A range of fiber pulling velocities was used, from 5 to 15 $mm.s^{-1}$.

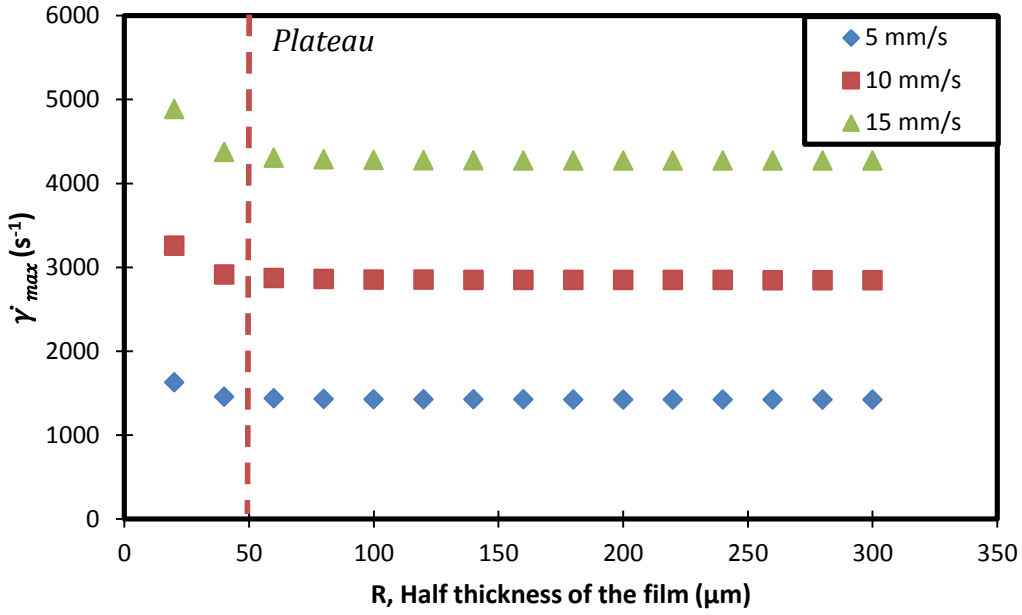

Figure 4.1: Maximum shear rate $\dot{\gamma}_{max}$ as a function of half thickness of the film R for different fiber pulling velocities.

For film thickness larger than 100-200 µm, $\dot{\gamma}_{max}$ seems to reach a plateau (Figure 4.1). Therefore, a minimum value of 200 µm thickness was adopted. Preliminary experiments were performed to determine the required initial value of the composite films. We found that the initial thickness of the composite (250 µm + 250 µm) yield to a thickness of 215 µm for the composite after melting. Some relaxation studies used sample thicknesses to match the diameter of the fiber but, in most other studies, the thickness of the film ranges between 100 and 500 µm [14] [13] [83], in accordance with our experiments.

A velocity of pulling of 5-10 mm.s^{-1}, over distances between 5 and 10 mm has been used, that is in accord with other studies [14] [13] [83]. Small differences in velocity of pulling do not have a strong effect on the obtained morphology [14]. The diameter of the glass fibers used is 17 µm which is similar to those used in previous relaxation studies [14] [13] [83].

Note that $\dot{\gamma}_{max}$ decreases very rapidly with distance from the fiber (Figure 4.2). Therefore, we expect most of the flow effect at very small distances from the fiber.

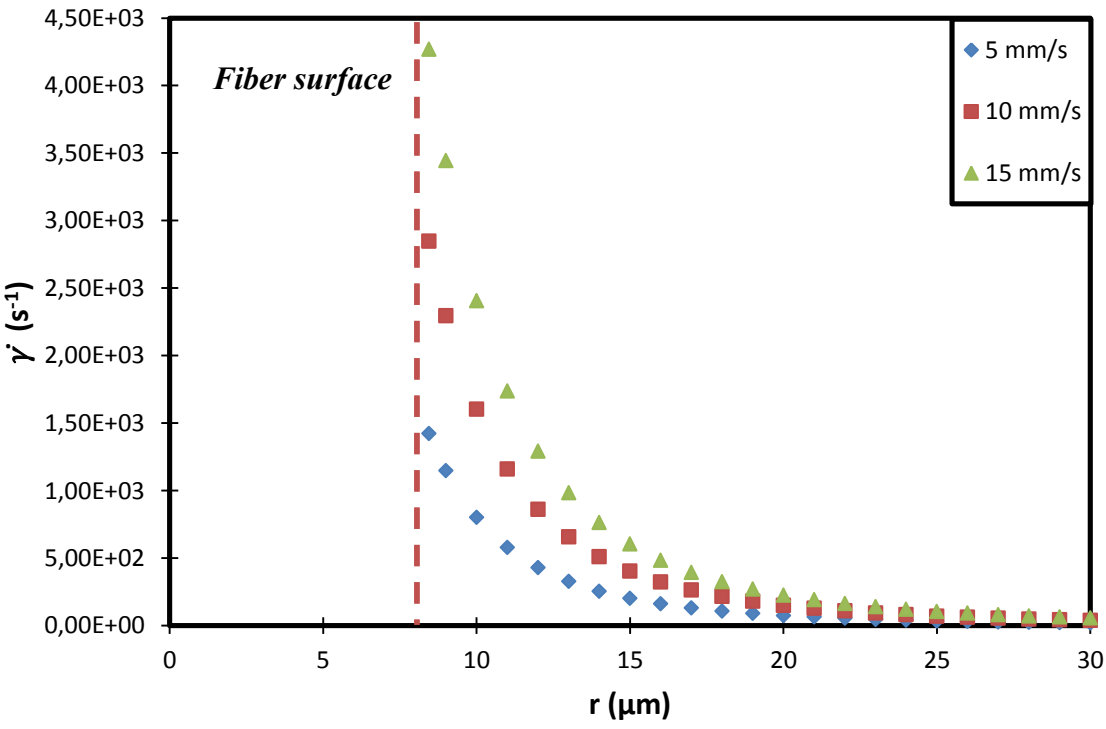

Figure 4.2: Shear rate $\dot{\gamma}$ as a function of radial distance r from the fiber axis for different fiber pulling velocities

4.2 Control experiment in quiescent conditions

For flow-relaxation experiments, it is required that the fibers themselves not induce a transcrystalline layer in the absence of flow, i.e., under quiescent conditions. Preliminary experiments were performed with fibers #FGI Flexstrand 110EM13347 and #EC13 272 Z20 T6M H9 Vetrotex and it was found that neither induced a transcrystalline layer on the surface of the fiber. Glass fiber #FGI Flexstrand 110EM13347, which was used in most experiments, is shown in Figure 4.3.

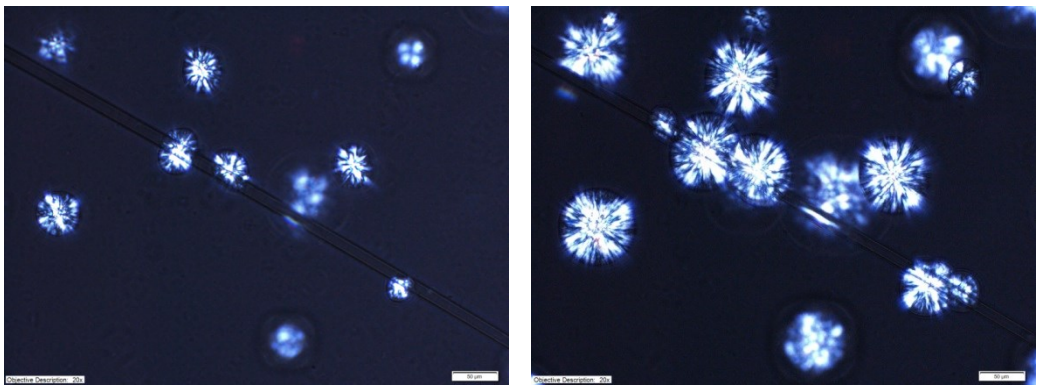

Figure 4.3: FiberGlassIndustries #FGI Flexstrand 110EM13347 glass fiber – iPP composite under quiescent conditions at Tc = 135°C and after isothermal crystallization time of 15 min (left) and 25 min (right).

It is worth noting that the phenomenon of transcrystallization has never been demonstrated with uncoated glass fibers [96] [97], while some coated glass fibers with acid-modified polypropylene (AMPP) have been shown to induce transcrystallization [98].

4.3 Morphological observations

Figure 4.4 shows the typical morphology development for a fiber pull experiment. The iPP homopolymer sample was sheared at T_{pull} = 172.5°C and relaxed at T_R = 172.5°C for t_R = 40 minutes before being cooled down to T_c = 135°C, where it was allowed to crystallize for 15 minutes.

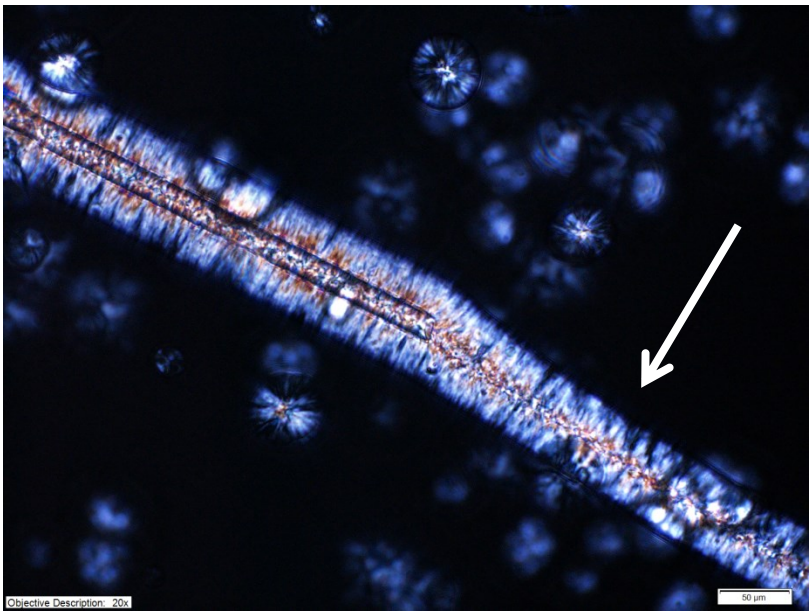

Figure 4.4: Cylindritic morphology around the pulled glass fiber #FGI Flexstrand 110EM13347 in the iPP matrix after a shear relaxation experiment with parameters $T_{pull} = T_R$ = 172.5°C, t_R = 40 min and T_c = 135°C. Image was taken at 15 min of crystallization at T_c = 135°C.

Several observations can be made in Figure 4.4. First, we observe a highly oriented crystalline growth on the fiber surface which, according to section 4.2, cannot be due to transcrystallinity. Therefore, it must be due to the applied shear flow. This is further confirmed by examining the morphology in the wake of the fiber (see white arrow in Figure 4.4).

At distances farther away from the fiber surface, only spherulites are growing. This is explained by the rapid decrease of shear rate as distance from the fiber surface is increased (Figure 4.2). This morphology is what would be obtained under quiescent conditions. Note that the cylindritic morphology and the bulk spherulites are developing at the same linear growth rate, which indicates that the linear growth rate is not affected by the previous flow history [14].

Additionally, when the fiber was pulled, a birefringent zone was briefly observed around the fiber [14]. Isayev pointed out that this temporary birefringence quickly disappears whereas the effect of the flow may be conserved during longer times [8].

4.4 Determination of critical holding time t*

The presence of high nucleation density or cylindritic morphology around the fiber is a clear indicator of residual perturbation in the polymer melt implying that complete reequilibration has not been attained. The critical holding time t* needed to erase the effect of the applied flow has been determined with a trial-and-error procedure. t* is calculated as the mean value of two times. One time corresponds to the maximum holding time at T_R for which some cylindritic morphology is still observed upon cooling to T_c. The other time corresponds to the minimum time for which only a spherulitic morphology is observed.

An example of the process of decay of high nucleation density with increasing relaxation time t_R at fixed relaxation temperature T_R is shown in Figure 4.5. All samples were subjected to the same thermomechanical history except for the duration of the relaxation time t_R.

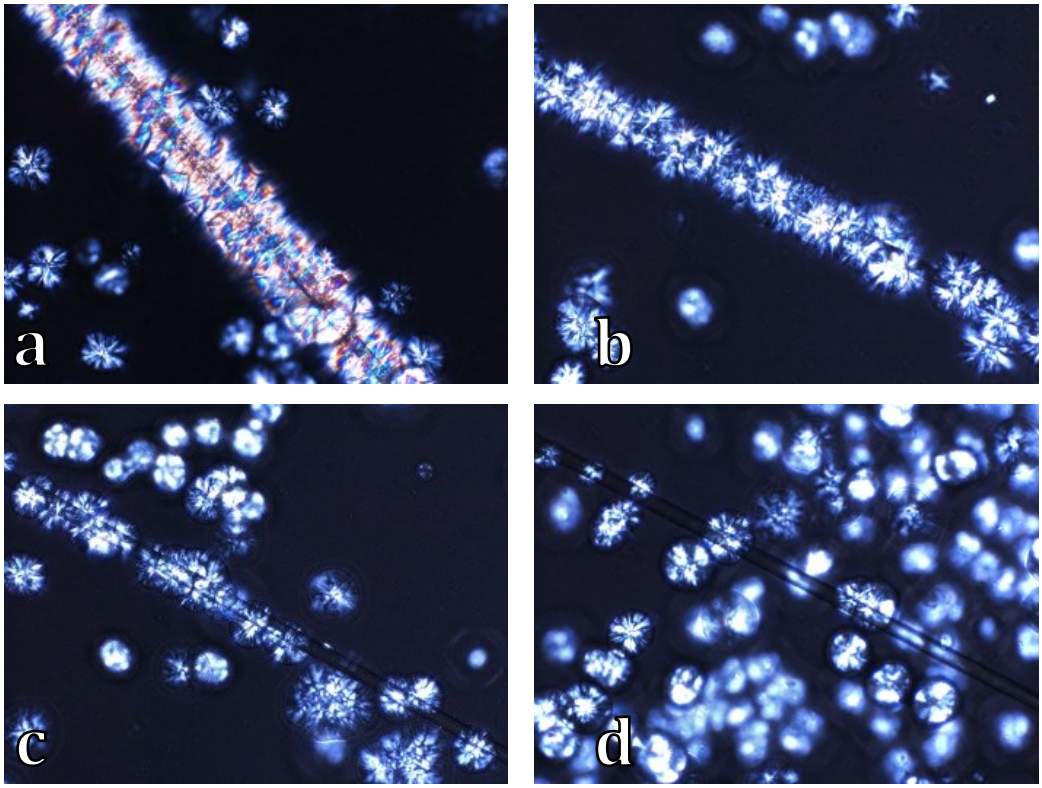

Figure 4.5: Morphological evolution of iPP samples with $T_{pull} = T_R = 180°C$ and isothermally crystallized at $T_c = 135°C$ for relaxation times of (a) $t_R = 5$ s, (b) $t_R = 10$ min, (c) $t_R = 15$ min, (d) $t_R = 20$ min.

A progressive disappearance of the oriented nucleation on the fiber with increasing t_R is clearly visible in Figure 4.5, (a) through (c), implying a partial disappearance of flow induced precursors. Once 20 min of relaxation have been reached (Figure 4.5 (d)), all the flow-memory was erased leaving only spherulites dispersed throughout the bulk.

In order to account for possible inhomogeneity of the glass fiber coating, we examined the morphology in different areas of the sample and repeated some experiments as needed to confirm the results. Other authors have also pointed out that the observation area needs to be carefully chosen in crystallization experiments after shear treatment on polypropylene [88].

4.5 Relaxation experiments

Two types of experiments were performed: one with $T_{pull} = T_R$ as the thermomechanical protocol (procedure 1), and the other with $T_{pull} \neq T_R$ but with T_{pull} always fixed (procedure 2).

4.5.1 $T_{pull} = T_R$ experiments

To construct morphological maps, each experiment was classified according to the final structure (Figure 4.6 for iPP, Figure 4.7 for RACO3 and Figure 4.8 for RACO7). Selection criteria were based on Figure 4.5: (a) which shows cylindritic morphology was considered as “highly nucleated”, (c) with a decreased nucleation activity along the fiber was regarded as “low nucleated”, (d) showing only spherulitic morphology was considered as “spherulitic”.

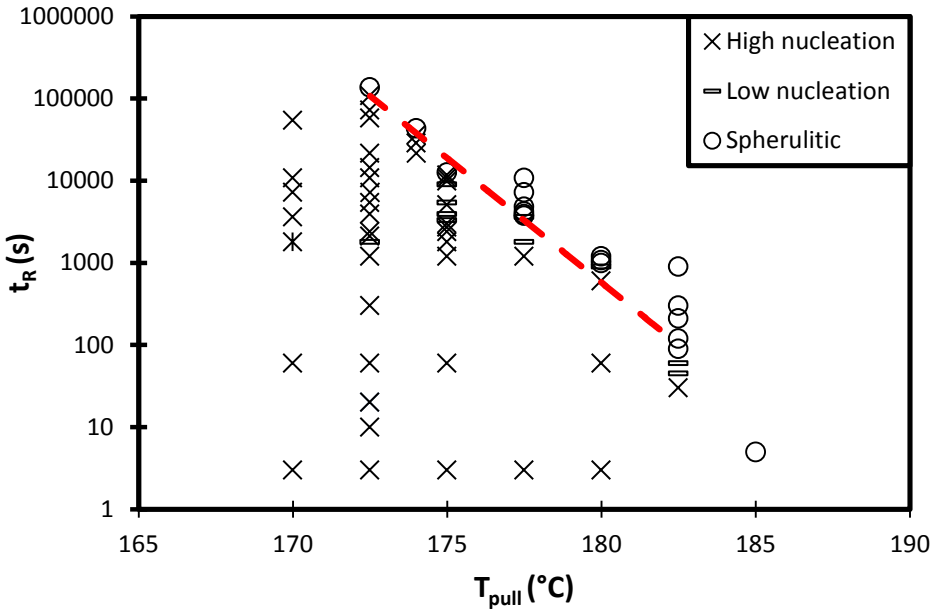

Figure 4.6: iPP morphological map for relaxation experiment with $T_{pull} = T_R$. Dashed line fits the values of critical relaxation times t*.

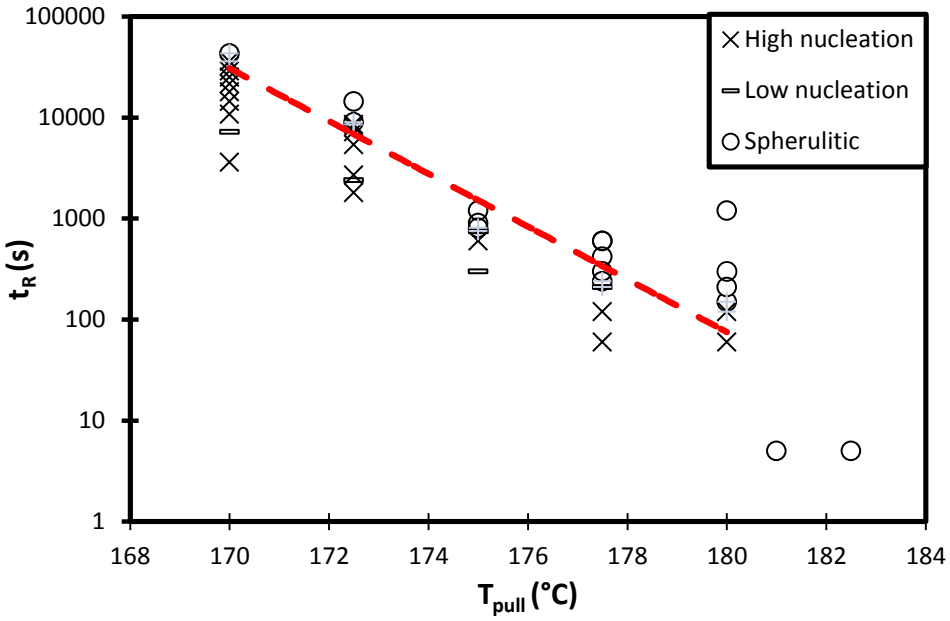

Figure 4.7: RACO3 morphological map for $T_{pull} = T_R$. Dashed line fits the values of critical relaxation times t*.

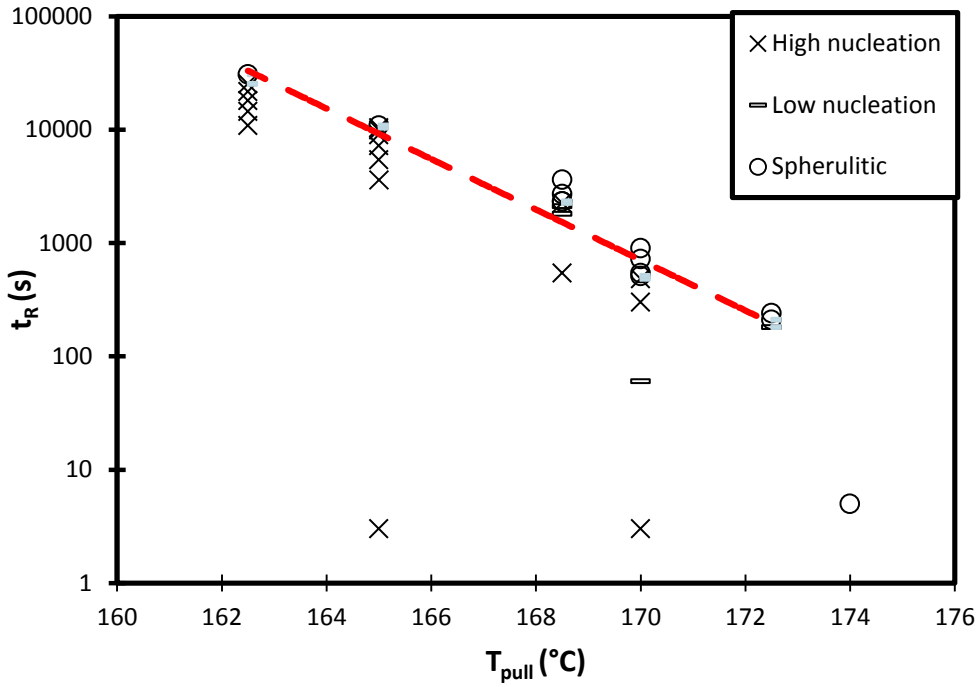

Figure 4.8: RACO7 morphological map for $T_{pull} = T_R$. Dashed line fits the values of critical relaxation times t*.

Critical times t* for each relaxation temperature are fitted by a red dashed straight line and show a strong dependence of critical holding time t* on the relaxation temperature T_R. The critical holding times t* for experiments in which $T_{pull} = T_R$ are shown Table 4.1. At each temperature, two values of time are reported. The first one corresponds to the maximum holding time for which some cylindritic morphology is observed. Instead, the second value corresponds to the minimum time for which only a spherulitic morphology is observed. This second value of t* has been confirmed for each relaxation temperature T_R, by using a somewhat longer relaxation time and ensuring that the morphology is spherulitic as well.

Table 4.1: Critical holding times, t* (in s), for complete disappearance of the cylindritic morphology for $T_{pull} = T_R$.

T_R (°C)	iPP	RACO3	RACO7
185	< 5		
182.5	60-90		
180	900-990	120-150	
177.5	3600-3750	210-240	
175	11700-12600	750-810	
174	36000-43200		
172.5	108000-136800	8520-9000	180-210
170		36000-43200	480-510
168.5			2250-2325
165			10320-10800
162.5			30600-39600

A first observation on the critical holding times indicates very clearly that the lifetime of nucleation precursors is a highly sensitive function of relaxation temperature. As an example, the time required to fully erase the nucleation activity along the fiber for the iPP increases from 16 min 30 s at 180°C to more than 30 hours at 172.5°C. In one of Alfonso's work on poly(1-butene) [14], he observed an increase of the critical times of around 3 orders of magnitude when the relaxation temperature was decreased by 10°C. Ziabicki and Alfonso [99] considered a complex model based on crystal nucleation theory to explain these longer times of relaxation.

With increasing ethylene content, lower temperature of relaxation T_R must be used to obtain similar values of critical relaxation time t*. One notes that it is reasonable to assume that nominal melting temperature decrease with an increase of defect content.

Apparent activation energies, E_a (in J.mol^{-1}), for the complete disappearance of flow induced structures of **1175 ± 58 kJ.mol^{-1}**, **1004 ± 50 kJ.mol^{-1}** and **858 ± 42 kJ.mol^{-1}** were obtained for iPP, RACO3 and RACO7, respectively.

An Arrhenius plot based on the equation below was used to calculate the apparent activation energy E_a (Figure 4.9):

$$\ln(t^*) = \ln(A) - \frac{E_a}{R}\left(\frac{1}{T}\right) \tag{6}$$

where t* (in s) is the critical relaxation time, A is a pre-exponential factor, R is the gas constant (8.314 J.K^{-1}.mol^{-1}) and T is the absolute temperature (in Kelvin).

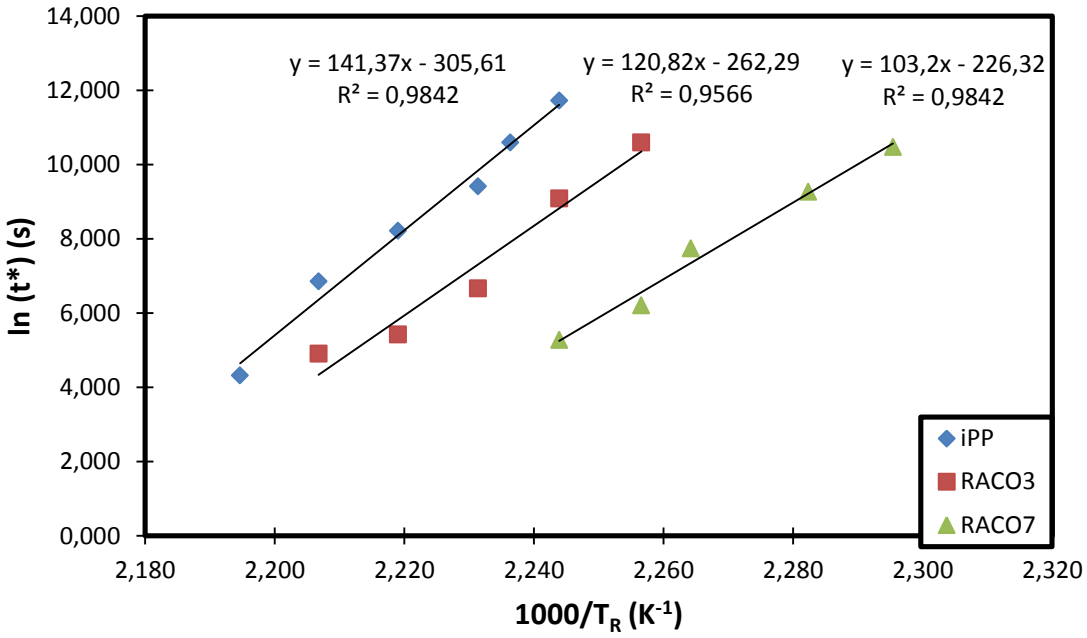

Figure 4.9: Critical holding times as a function of relaxation temperature for iPP, RACO3 and RACO7 with $T_{pull} = T_R$.

4.5.2 $T_{pull} \neq T_R$ experiments (T_{pull} fixed)

Using the same criteria as in section 4.5.1, three morphological maps were constructed for $T_{pull} \neq T_R$, with always T_{pull} fixed. (Figure 4.10 for iPP, Figure 4.11 for RACO3 and Figure 4.12 for RACO7). The pulling temperatures were, respectively, 174°C, 170°C and 162.5°C for iPP, RACO3 and RACO7. These temperatures were chosen using the critical relaxation times t* as a function of relaxation temperature T_R, by estimating the value of T_R that would yield a t* on the order of several hours (approximately ten hours).

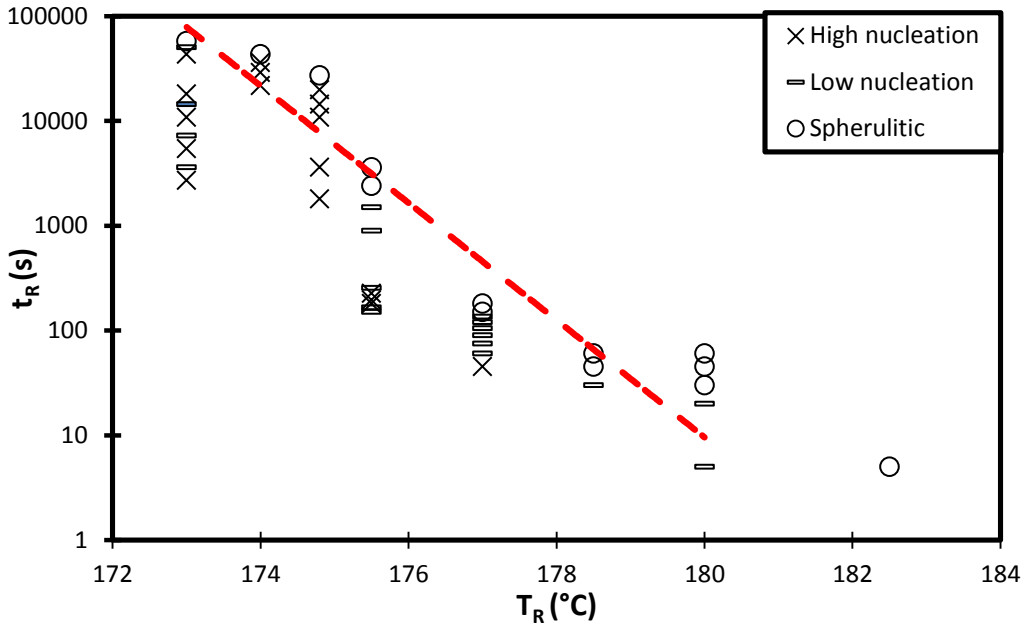

Figure 4.10: iPP morphological map for relaxation experiment with $T_{pull} \neq T_R$ (T_{pull} = constant). Dashed line fits the values of critical relaxation times t*.

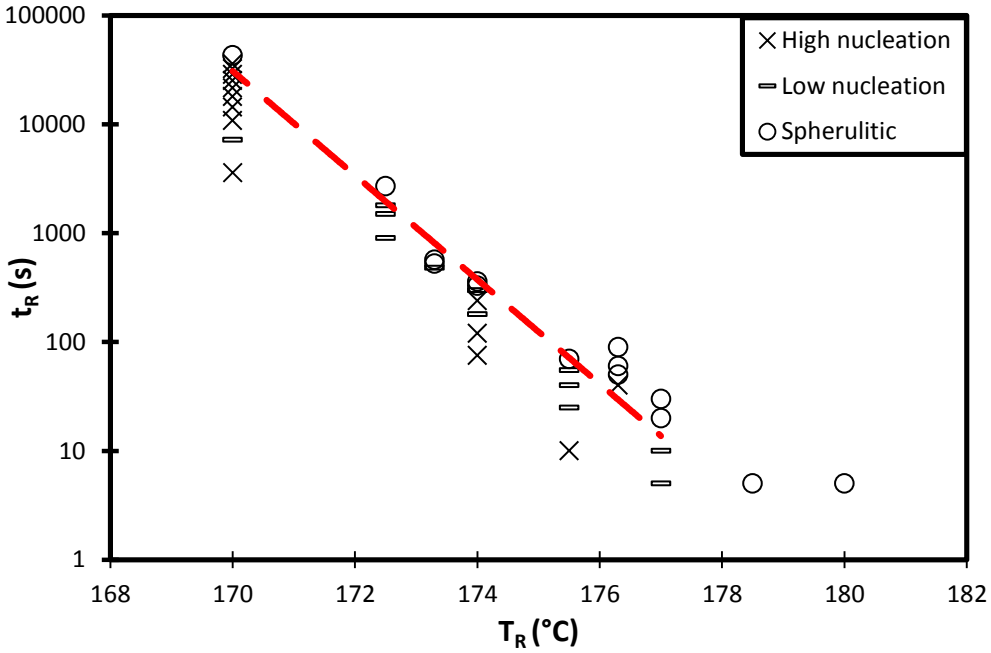

Figure 4.11: RACO3 morphological map for relaxation experiment with $T_{pull} \neq T_R$ (T_{pull} = constant). Dashed line fits the values of critical relaxation times t*.

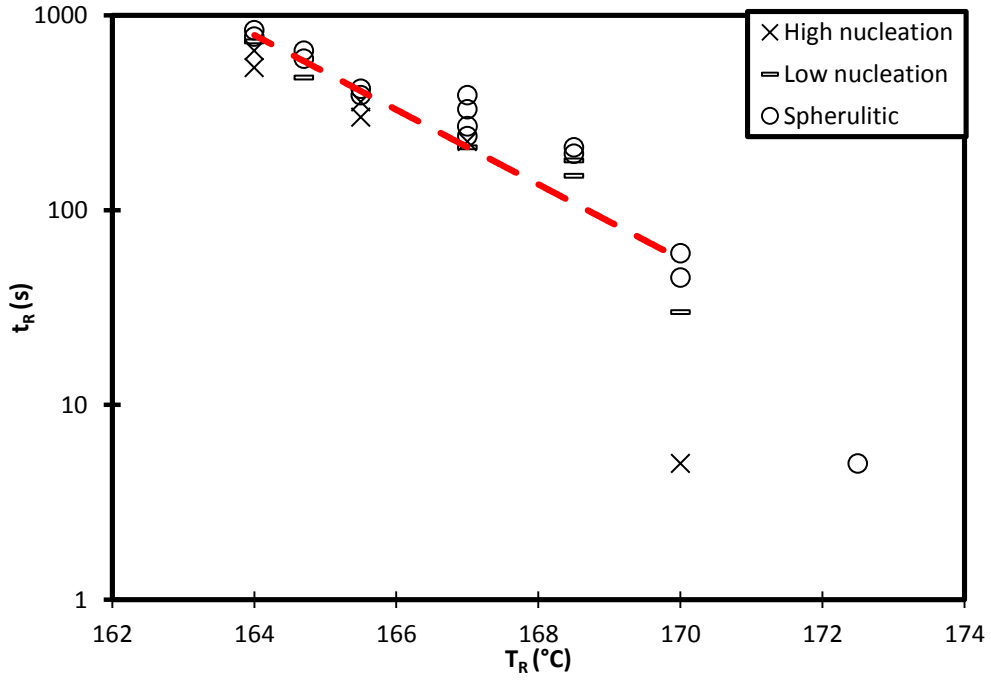

Figure 4.12: RACO7 morphological map for relaxation experiment with $T_{pull} \neq T_R$ (T_{pull} = constant). Dashed line fits the values of critical relaxation times t*.

The critical holding times t* for experiments in which $T_{pull} \neq T_R$ are reported in Table 4.2. The first value corresponds to the maximum holding time for which some cylindritic morphology is observed, and the second one corresponds to the minimum time for which only a spherulitic morphology is observed. Similar to the experiments with $T_{pull} = T_R$, the critical holding times indicate clearly that the lifetime of nucleation precursors is a highly sensitive function of relaxation temperature.

Here, the time required to fully erase the nucleation activity along the fiber for the iPP increases from 30 s at 180°C to 12 hours at 174°C. It should be noted that a disproportionate value t* value for RACO7 at T_R=162.5C was found and was not included later in the fitting to obtain apparent energies of activation E_a. Moreover, the critical time required to completely erase the memory of flow on the morphology development changes dramatically if $T_{pull} \neq T_R$. As an example, for the iPP, the critical time increase from around 285 s when T_R = 175°C ($T_{pull} \neq T_R$) to 3h 30min when T_R = 175.5°C ($T_{pull} = T_R$).

Table 4.2: Critical holding times, t* (in s), for complete disappearance of the cylindritic morphology for $T_{pull} \neq T_R$ (T_{pull} = constant).

T_R (°C)	iPP	RACO3	RACO7
180	20-30		
178.5	30-45		
177	135-150	10-20	
176.3		40-50	
175.5	1500-2400	55-70	
174.8	19800-27000		
174	36000-43200	300-330	
173.3		480-525	
173	50400-57600		
172.5		1800-2700	
170		36000-43200	30-45
168.5			180-195
167			225-240
165.5			360-390
164.7			480-600
164			735-780
162.5			30600-39600

An Arrhenius plot based on the equation (6) was used. Values of **2161 ± 108 kJ.mol^{-1}**, **1823 ± 91 kJ.mol^{-1}** and **707 ± 35 kJ.mol^{-1}** were obtained for iPP, RACO3 and RACO7, respectively. The strong effect of the relaxation temperature can be appreciated by comparing the apparent activation energies determined. For the iPP with $T_{pull} = T_R$, the activation energy is 1175 kJ.mol^{-1}, whereas with $T_{pull} \neq T_R$ (T_{pull} is fixed) the value strongly increases to reach 2161 kJ.mol^{-1}.

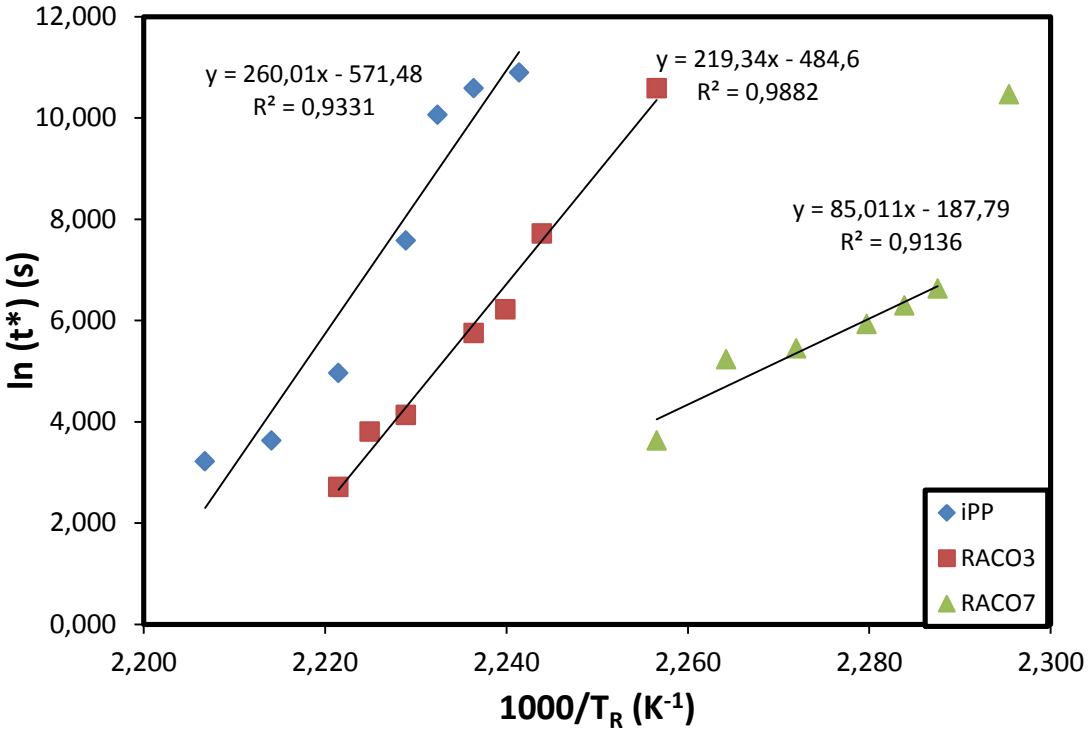

Figure 4.13: Critical holding times as a function of relaxation temperature for iPP, RACO3 and RACO7 with $T_{pull} \neq T_R$ (T_{pull} = constant).

4.6 Discussion

4.6.1 Discussion on activation energies

The activation energies E_a obtained for iPP in our study are somewhat larger than E_a for iPP found in previous studies, which were typically in the range of 150 and 300 kJ.mol^{-1}. The cause of discrepancy is not specifically known, but the conditions used in the relaxation experiments could be at the origin of this difference.

Indeed, for relaxation studies of iPB, Janeschitz-Kriegl [15] found a value of 224 $kJ.mol^{-1}$ which is half the value of 500 $kJ.mol^{-1}$ found by Alfonso [14]. Janeschitz-Kriegl attributed the difference in criteria for determining t* as the possible cause. Furthermore, the range of relaxation temperatures was not the same: Janeschitz-Kriegl [15] relaxation temperatures of 150-170°C whereas Alfonso used 125-150°C.

Upon careful examination of the literature, one can find that the experimental parameters can vary between different studies. For example, Alfonso's group does use the same fiber pull procedure and complete disappearance criteria as in this thesis. However, the range temperature of relaxation of 190-210°C differs from ours that is 172.5-185°C. Also, Janeschitz-Kriegl [8] [15] and Isayev [71] used duct flow technique and a different range of T_R. In addition, their criteria is based on relative decay of precursors while in our study, we looked for a complete disappearance. Finally, Cavallo [16] does use similar temperatures to ours, but with a rotational device and using partial disappearance as their criteria.

4.6.2 Discussion on detachment of single stem

Azzurri [13] associates the apparent activation energy with a characteristic chain stem length L_S that detaches from the precursor when melting. Therefore, a progressive disappearance of cylindritic morphology can proceed through a consecutive detachment of chain stems. Once detached, the chain will progressively return to the polymer melt.

The length of the detaching stem L_s can be determined as [13]:

$$L_s = \frac{E_a}{\Delta H_m} \times L_u$$

where L_u corresponds to the length of the repeating unit along the c-axis in the corresponding crystalline lattice (0.22 nm [100]). E_a, is the apparent activation energy of flow induced precursors and ΔH_m, is the melting enthalpy of the isotactic polypropylene (8.7 kJ.mol^{-1} [101]). The thermodynamic melting enthalpy of 8.7 kJ.mol^{-1} of the perfect 100% isotactic polypropylene crystal was used [92]. This value has been used in previous studies, for both iPP and its copolymers [41] [92]. The calculated values of detaching stem lengths are reported in Table 4.3.

Table 4.3: Values of stem length

	L_S (nm)	
	$T_{pull} = T_R$	$T_{pull} \neq T_R$
iPP	29.7	54.6
RACO3	25.4	46.1
RACO7	21.7	17.8

Our calculated L_S are larger than those found for iPP in previous studies, which were ~ 7 nm [13]. However, the L_S found for $T_{pull} = T_R$ experiments are similar to those found with POE and PB, which ranged from 8 nm for polystyrene to 22 nm for polyoxyethylene and polybutene [13]. The reasons for these differences have been discussed above.

4.6.3 Effect of comonomers

For experiments with $T_{pull} = T_R$, the apparent activation energies E_a and detaching stem lengths L_S decrease with increasing ethylene content. One knows that the ethylene units in polypropylene play a major role in the chain, by acting as perturbations of crystalline structure [41]: crystallinity, melting and crystallization temperatures decrease with increasing comonomer content (up to 21 mol %) [102] . Therefore, the decrease in activation energy values by increasing ethylene content seems reasonable.

CHAPTER 5: CONCLUSION

Here we studied the relaxation characteristics of flow induced precursors for a series of isotactic polypropylene and random propylene-ethylene copolymers (3.4 and 7.3% ethylene content) using a fiber pull experimental protocol.

In general, we found that the lifetime of flow induced precursors t* decreased with increasing temperature and that they were able to survive for several hours at temperatures even above their nominal melting temperature. Also, the apparent energies of activation E_a for disappearance of these precursors and the detachment of stem length L_S was found to decrease with increasing ethylene content. This may be attributed to ethylene units in polypropylene which act as perturbations of the crystalline structure. The values of E_a for iPP in our experiments were larger than those found in literature and the cause of discrepancy is not known. Several possible causes, such the selection criteria of t* or the specific ranged relaxation temperatures investigated were discussed. The detachment of stem length L_S for $T_{pull} = T_R$ is within the range that has previously been found for polymers such as PEO and PB, although they are higher than those reported earlier for iPP. In the case of $T_{pull} \neq T_R$, the L_S values for iPP and RACO3 exceeded those previously found. Further work needs to be done to investigate the effect of using a fixed pulling temperature and of the specific value of T_{pull} relative to the nominal melting temperature.

BIBLIOGRAPHY

[1] L. Bove and M. R. Nobile, "Shear-Induced Crystallization of Isotactic Poly(1-butene)," *Macromolecules Symposium,* vol. 185, pp. 135-147, 2002.

[2] F. Jay, J. Haudin and B. Monasse, "Shear-induced crystallization of polypropylenes: effect of molecular weight," *Journal of Materials Science,* vol. 34, p. 2089 – 2102, 1999.

[3] J. Baert and P. Van Puyvelde, "Effect of molecular and processing parameters on the flow-induced crystallization of poly-1-butene. Part 1: Kinetics and morphology," *Elsevier Polymer,* vol. 47, pp. 5871-5879, 2006.

[4] C. Duplay, B. Monasse, J.-M. Haudin and J.-L. Costa, "Shear-induced crystallization of polypropylene: influence of molecular structure," *Polymer International,* vol. 48, pp. 320-326, 1999.

[5] R. G. Alamo, D. L. VanderHart, M. R. Nyden and L. Mandelkern, "Morphological Partitioning of Ethylene Defects in Random Propylene-Ethylene Copolymers," *Macromolecules ,* vol. 33, pp. 6094-6105, 2000.

[6] Y. Zhao, K. Hayasaka, G. Matsuba and H. Ito, "In Situ Observations of Flow-

Induced Precursors during Shear Flow," *Macromolecules,* vol. 46, p. 172−178, 2013.

[7] L. Balzano, N. Kukalyekar, S. Rastogi, G. W. M. Peters and J. C. Chadwick, "Crystallization and Dissolution of Flow-Induced Precursors," *Physical Review Letters,* vol. 100, no. 4, pp. 048302-048304, 2008.

[8] A. Isayev, T. Chan, K. Shimojo and M. Gmerek, "Injection Molding of Semicrystalline Polymers. I. Material Characterization," *Journal of Applied Polymer Science ,* vol. 55, pp. 807-819, 1995.

[9] J. Kornfield, G. Kumaraswamy and A. Issaian, "Recent Advances in Understanding Flow Effects on Polymer Crystallization," *Industrial & Engineering Chemistry Research,* vol. 41, pp. 6383-6392, 2002.

[10] R. H. Somani, B. S. Hsiao, A. Nogales, S. Srinivas, A. H. Tsou, I. Sics, F. J. Balta-Calleja and T. A. Ezquerra, "Structure Development during Shear Flow-Induced Crystallization of i-PP: In-Situ Small-Angle X-ray Scattering Study," *Macromolecules,* vol. 33, pp. 9385-9394, 2000.

[11] G. Kumaraswamy, R. Verma and J. Kornfield, "Novel flow apparatus for investigating shear-enhanced crystallization and structure development in semicrystalline polymers," *American Institute of Physics,* vol. 70, no. 4, pp. 2097-2104, 1999.

[12] R. H. Somani, L. Yang and B. S. Hsiao, "Precursors of primary nucleation induced by fow in isotactic polypropylene," *Elsevier Physica A,* vol. 304, pp. 145-157,

2002.

[13] F. Azzurri and G. Alfonso, "Insights into Formation and Relaxation of Shear-Induced Nucleation Precursors in Isotactic Polystyrene," *Macromolecules,* vol. 41, pp. 1377-1383, 2008.

[14] F. Azzurri and G. C. Alfonso, "Lifetime of Shear-Induced Crystal Nucleation Precursors," *Macromolecules,* vol. 38, pp. 1723-1728, 2005.

[15] H. Janeschitz-Kriegl and G. Eder, "Shear Induced Crystallization, a Relaxation Phenomenon in Polymer Melts: A Re-Collection," *Journal of Macromolecular Science, Part B: Physics,* vol. 46, p. 591–601, 2007.

[16] D. Cavallo, F. Azzurri, L. Balzano, S. Funari and G. Alfonso, "Flow Memory and Stability of Shear-Induced Nucleation Precursors in Isotactic Polypropylene," *Macromolecules,* vol. 43, p. 9394–9400, 2010.

[17] J.-W. Housmans, G. Peters and H. Meijer, "Flow-induced crystallization of propylene/ethylene random copolymers," *Journal of Thermal Analysis and Calorimetry ,* vol. 98, pp. 693-705, 2009.

[18] M. Wolkowicz, "Nucleation and crystal-growth in sheared poly(1-butene) melts," *Journal of Polymer Science Part C- Polymer Symposium,* vol. 63, pp. 365-382, 1977.

[19] J. J. De Yoreo and P. G. Vekilov, "Principles of Crystal Nucleation and Growth," *Reviews in mineralogy and geochemistry ,* vol. 54, pp. 57-93, 2003.

[20] C. Duval, "Polypropylènes (PP)," *Techniques de L'ingénieur,* 2004.

[21] D. C. Bassett, A. Keller and S. Mitsuhashi, "New features in polymer crystal growth from concentrated solutions," *Journal of Polymer Science Part A: General Papers,* vol. 1, no. 2, p. 763–788, 1963.

[22] G. Patel and R. Patel, "Growth Mechanism of Polymer Hedrites," *European Polymer Journal,* vol. 6, pp. 657-662, 1970.

[23] A. M. Cunha and S. Fakirov, Structure Development During Polymer Processing, Springer, 2000.

[24] D. B. Malpass and E. Band, Introduction to Industrial Polypropylene: Properties, Catalysts Processes, John Wiley & Sons , 2012.

[25] J. Wünsch, Polystyrene: Synthesis, production and applications, Woodhead Publishing Limited, 2000.

[26] G. Natta and C. P., "Structure and properties of isotactic polypropylene," *Nuovo Cimento,* vol. 15, no. 1 Supplement, pp. 40-51, 1960.

[27] P. De Santis, E. Giglio, A. M. Liquori and A. Ripamonti, "Stability of helical conformations of simple linear polymers," *Journal of Polymer Science Part A: General Papers,* vol. 1, no. 4, p. 1383–1404, 1963.

[28] H. D. Keith, F. J. Padden, N. M. Walter and H. W. Wyckoff, "Evidence for a Second Crystal Form of Polypropylene," *Journal Of Applied Physics,* vol. 30, no. 10, pp. 1485 - 1488, October 1959.

[29] E. J. Addink and J. Beintema, "Polymorphism of Crystalline Polypropylene," *Journal of Polymer,* vol. 2, pp. 185-193, 1962.

[30] R. G. Alamo, M.-H. Kim, M. J. Galante, J. R. Isasi and L. Mandelkern, "Structural and Kinetic Factors Governing the Formation of the Gamma Polymorph of Isotactic Polypropylene," *Macromolecules,* vol. 32, pp. 4050-4064, 1999.

[31] S. V. Meille, S. Brückner and P. W., "y-Isotactic Polypropylene. A Structure with Nonparallel Chain," *Macromolecules ,* vol. 23, no. 18, pp. 4114-4121, 1990.

[32] F. Candia, P. S. G. Iannelli and V. Vittoria, "Crystallization of oriented smectic polypropylene I. Thermally induced crystallization," *Colloid and Polymer Science,* vol. 266, no. Issue 7, pp. 608-613, 1988.

[33] E. A. Campo, Industrial Polymers, Hanser Gardner Publications, 2007.

[34] C. De Rosa, F. Auriemma, T. Circelli and R. M. Waymouth, "Crystallization of the R and ç Forms of Isotactic Polypropylene as a Tool To Test the Degree of Segregation of Defects in the Polymer Chains," *Macromolecules,* vol. 35, pp. 3622-3629, 2002.

[35] C. Rosa, F. Auriemma, G. Talarico and O. Ballesteros, "Structure of Isotactic Propylene-Pentene Copolymers," *Macromolecules ,* vol. 40, pp. 8531-8532, 2007.

[36] K. Jeon, H. Palza, R. Quijada and R. Alamo, "Effect of comonomer type on the crystallization kinetics and crystalline structure of random isotactic propylene 1-alkene copolymers," *Elsevier Polymer,* vol. 50, p. 832–844, 2009 .

[37] D. Mileva, R. Androsch, D. Cavallo and G. C. Alfonso, "Structure formation of random isotactic copolymers of propylene and 1-hexene or 1-octene at rapid cooling," *European Polymer Journal ,* vol. 48, p. 1082–1092, 2012.

[38] C. De Rosa, F. Auriemma, P. Vollaro, L. Resconi, S. Guidotti and I. Camurati, "Crystallization Behavior of Propylene-Butene Copolymers: The Trigonal Form of Isotactic Polypropylene and Form I of Isotactic Poly(1-butene)," *Macromolecules ,* vol. 44, p. 540–549, 2011.

[39] C. a. m. o. p. r. c. H. n. a. b.-n. agents, "Papageorgiou, Dimitrios G. ; Papageorgiou, George Z. ; Bikiaris, Dimitrios N. ; Chrissafis, Konstantinos," *European Polymer Journal,* vol. 49, no. 6, p. 1577–1590, 2013 .

[40] C. De Rosa, F. Auriemma, V. Vintia, A. Grassi and M. Galimberti, "Polymorphism of syndiotactic polypropylene in copolymers of propylene with ethylene and 1-butene," *Elsevier Polymer,* vol. 39, no. 25, p. 6219–6226, 1998.

[41] M.-H. Kim, R. G. Alama and J. S. Lin, "The Cocrystallization Behavior of Binary Blends of lsotactic Polypropylene and Propylene-Ethylene Random Copolymers," *Polymer Engineering & Science,* vol. 39, no. 11, pp. 2117-2131, 1999.

[42] I. L. Hosiera, R. G. Alamo and J. Lin, "Lamellar morphology of random metallocene propylene copolymers studied by atomic force microscopy," *Elsevier Polymer ,* vol. 45, p. 3441–3455, 2004.

[43] G. Pompe and E. Mäder, "Experimental detection of a transcrystalline interphase in glass-fibre/polypropylene composites," *Composites Science and Technology,* vol. 60, pp. 2159-2167, 2000.

[44] T. Chan and A. Isayev, "Quiescent Polymer Crystallization: Modeling and Measurements," *Polymer Engineering and Science,* vol. 34, no. 6, pp. 461 - 471,

1994.

[45] C. Wang and L. M. Hwang, "Transcrystallization of PTFE Fiber/PP Composites (I) Crystallization Kinetics and Morphology," *Journal of Polymer Science: Part B: Polymer Physics,* vol. 34, pp. 47-56, 1996.

[46] C. Wang and C.-R. Liu, "Transcrystallization of PTFE Fiber/PP Composites - III. Effect of Fiber Pulling on the Crystallization Kinetics," *Journal of Polymer Science: Part B: Polymer Physics,* vol. 36, p. 1361–1370, 1998.

[47] O. Lee and M. Kamal, "Experimental Study of Post-Shear Crystallization of Polypropylene Melts," *Polymer Engineering and Science,* vol. 39, no. 2, pp. 236-248, February 1999.

[48] R. H. Somani, L. Yanga, L. Zhub and B. S. Hsiao, "Flow-induced shish-kebab precursor structures in entangled polymer melts," *Elsevier Polymer,* vol. 46, p. 8587–8623, 2005.

[49] R. Lagasse and B. Maxwell, "An Experimental Study of the Kinetics of Polymer Crystallization During Shear Flow," *Polymer Engineering and Science,* vol. 16, no. 3, pp. 189-199, 1976.

[50] C. Tribout, B. Monasse and J. Haudin, "Experimental Study of Shear-Induced Crystallization of an Impact Polypropylene Copolymer," *Colloid Polymer Science ,* vol. 247, no. 3, pp. 197-208, 1996.

[51] H. Janeschitz-Kriegl, E. Ratajski and M. Stadlbauer, "Flow as an effective promotor of nucleation in polymer melts: a quantitative evaluation," *Rheol Acta ,*

vol. 42, p. 355–364, 2003.

[52] H. Janeschitz-Kriegl and E. Ratajski, "Kinetics of polymer crystallization under processing conditions: transformation of dormant nuclei by the action of flow," *Elsevier Polymer ,* vol. 46, p. 3856–3870, 2005.

[53] S. Liedauer, G. Eder and H. Janeschitz-Kriegl, "On the Limitations of Shear Induced Crystallization in Polypropylene Melts," *International Polymer Processing,* vol. 3, pp. 243-250, 1995.

[54] P. Jerschow and H. Janeschitz-Kriegl, "On the development of oblong particles as precursors for polymer crystallization from shear flow: Origin of the so-called fine grained layers," *Rheologica Acta,* vol. 35, no. 2, p. 127–133, 1996.

[55] P. Jerschow and H. Janeschitz-Kriel, "The role of long molecules and nucleating agents in shear induced crystallization of isotactic polypropylenes," *International Polymer Processing,* vol. 12, no. 1, pp. 72-77, 1997.

[56] H. Janeschitz-Kriegl, "How to understand nucleation in crystallizing polymer melts under real processing conditions," *Colloid Polymer Science,* vol. 281, pp. 1157-1171, 2003.

[57] M. R. Mackley and A. Keller, "Flow induced polymer-chain extension and its relation to fibrous crystallization," *Philosophical Transactions of the Royal Society of London Series a-Mathematical Physical and Engineering Sciences ,* vol. 278, no. 29, pp. 30-66, 1975.

[58] A. Keller and H. Kolnaar, "Flow-Induced Orientation and Structure Formation,"

Wiley-VCH, New York, 1997.

[59] A. J. Pennings, J. Smook, J. D. Boer, S. Gogolewski and P. F. V. Hutten, "Process of preparation of ultra-high strength polyethylene fibers," *Pure and Applied Chemistry,* vol. 55, no. 5, p. 777—798, 1983.

[60] M. R. Mackley and A. Keller, "Flow Induced Polymer Chain Extension and Its Relation to Fibrous Crystallization," *Philosophical Transactions of the Royal Society of London. Series A, Mathematical and Physical Sciences,* vol. 278, no. 1276, pp. 29-66, February 27, 1975 .

[61] A. W. Monks, H. M. White and D. C. Bassett, "On shish-kebab morphologies in crystalline polymers," *Elsevier Science Polymer,* vol. 37, no. 26, pp. 5933-5936, 1996.

[62] H. M. White and D. C. Bassett, "On row structures, secondary nucleation and continuity in alpha-polypropylene," *Elsevier Science Polymer ,* vol. 39, no. 14, pp. 3211-3218, 1998.

[63] J.-M. Haudin, J.-M. André, G. M. B. Bellet and P. Navard, "Structure development during polymer processing. Morphological and crystallographic textures in polyethylene blown films," *La Revue de Métallurgie-CIT/Science et Génie des Matériaux,* Décembre 2002.

[64] I. L. Hay, M. Jaffe and K. F. Wissbrun, "A phenomenological model for row nucleation in polymers," *Journal of Macromolecular Science, Part B: Physics,* vol. 12 , no. 3, pp. 423-428, 1976.

[65] J. Dlugosz, D. Grubb, T. A. Keller and M. B. Rhodes, "Morphological verification of “Row nucleation” in isotactic polystyrene; evidence for single crystals within the bulk," *Journal of Material Science ,* vol. 7, pp. 142-147, 1972.

[66] N. Pogodina, V. Lavrenko, S. Srinivas and H. Winter, "Rheology and structure of isotactic polypropylene near the gel point: quiescent and shear-induced crystallization.," *Elsevier Polymer,* vol. 42, p. 9031–9043, 2011.

[67] R. Zhang, M. Min, Y. Gao, A. Lua and X. Yu, "Row nucleation phenomenon of Poly(phenylene sulfide) under shear condition," *Elsevier Materials Letters,* vol. 62, p. 1414–1417, 2008.

[68] J. Varga and J. Karger-Kocsis, "Direct evidence of row-nucleated cylindritic crystallization in glass fiber-reinforced polypropylene composites," *Polymer Bulletin,* vol. 30, pp. 105-110, 1993.

[69] M. R. Mackley, "Shish kebabs ; Hydrodynamic Factors Affecting Their Crystal Growth," *Colloid & Polymer Science,* vol. 253, pp. 373-379, 1975.

[70] M. Chellamuthu, D. Arora, H. H. Winter and J. P. Rothstein, "Extensional flow-induced crystallization of isotactic poly-1-butene using a filament stretching rheometer," *Journal of Rheology,* vol. 55, no. 4, pp. 901-920, July/August 2011.

[71] G. Eder, H. Janeschitz-Kriegl and S. Liedauer, "Crystallization process in quiescent and moving polymer melts under heat transfer conditions," *Progress in Polymer Science,* vol. 15, pp. 629-714, 1990.

[72] J. Braun, H. Wippel, G. Eder and H. Janeschitz-Kriegl, "Industrial Solidification

Processes in Polybutene-1. Part II - Influence of Shear Flow," *Polymer Engineering And Science,* vol. 43, no. 1, 2003.

[73] G. Kumaraswamy, A. Issaian and J. Kornfield, "Shear-Enhanced Crystallization in Isotactic Polypropylene.1. Correspondence between in Situ Rheo-Optics and ex Situ Structure Determination," *Macromolecules ,* vol. 32 , pp. 7537-7547, 1999.

[74] G. Kumaraswamy, J. Kornfield, F. Yeh and B. Hsiao, "Shear-Enhanced Crystallization in Isotactic Polypropylene. 3. Evidence for a Kinetic Pathway to Nucleation," *Macromolecules,* vol. 35, pp. 1762-1769, 2002.

[75] G. Kumaraswamy, R. Verma, J. Kornfield, F. Yeh and B. Hsiao, "Shear-Enhanced Crystallization in Isotactic Polypropylene. In-Situ Synchrotron SAXS and WAXD," *Macromolecules,* vol. 37, pp. 9005-9017, 2004.

[76] Y. Hayashi, G. Matsuba, Y. Zhao, K. Nishida and T. Kanaya, "Precursor of shish–kebab in isotactic polystyrene under shear flow," *Elsevier Polymer ,* vol. 50, p. 2095–2103, 2009.

[77] P. Van Puyvelde, F. Langouche and J. Baert, "Flow-induced crystallization in poly-1-butene: the shish-kebab transition," *International Journal of Material Forming,* vol. 1, no. Issue 1 Supplement, pp. 667-670, April 2008.

[78] B. Monasse, "Nucleation and anisotropic crystalline growth of polyethylene under shear," *Journal of Materials Science,* vol. 30, no. 19, p. 5002–5012, 1995.

[79] Z. Bashir, J. Odell and A. Keller, "Stiff and strong polyethylene with shish kebab morphology by continuous melt extrusion," *Journal Of Material Science,* vol. 21,

pp. 3993 - 4002, 1986.

[80] S. Vleeshouwers and H. E. H. Meijer, "A rheological study of shear induced crystallization," *Rheologica Acta,* vol. 35, no. 5, 1996.

[81] L. Bove and M. R. Nobile, "Shear Flow Effects on Polymer Melts Crystallization: Kinetics Features," *Macromolecules Symposium,* vol. 180, pp. 169-180, 2002.

[82] M. Nobile, L. Bove, E. Somma, I. Kruszelnicka and T. Sterzynski, "Rheological and Structure Investigation of Shear-Induced Crystallization of Isotactic Polypropylene," *Polymer Engineering And Science,* vol. 45, pp. 153-162, 2005.

[83] M. Gutiérrez, G. Alfonso, C. Riekel and F. Azzurri, "Spatially Resolved Flow-Induced Crystallization Precursors in Isotactic Polystyrene by Simultaneous Small- and Wide-Angle X-ray Microdiffraction," *Macromolecules ,* vol. 37, pp. 478-485, 2004.

[84] G. C. Alfonso and P. Scardigli, "Melt memory effects in polymer crystallization," *Macromolecular Symposia,* vol. 118, pp. 323-328, 1997.

[85] K. Kobayashi and T. Nagasawa, "Crystallization of Sheared Polymer Melts," *Macromolecules,* vol. B4, pp. 331-345, 1970.

[86] R. H. Somani, I. Sics and B. S. Hsiao, "Thermal Stability of Shear-Induced Precursor Structures in Isotactic Polypropylene by Rheo-X-ray Techniques with Couette Flow Geometry," *Journal of Polymer Science: Part B: Polymer Physics,* vol. 44, p. 3553–3570, 2006.

[87] G. Titomanlio and G. Marrucci, "Capillary Experiments of Flow Induced

Crystallization of HDPE," *AIChE Journal,* vol. 36, no. 1, pp. 13-18, 1990.

[88] E. Koscher and R. Fulchiron, "Influence of shear on polypropylene crystallization: morphology development and kinetics," *Elsevier Polymer,* vol. 43, p. 6931–6942, 2002.

[89] J. Moitzi and P. Skalicky, "Shear-induced crystallization of isotactic polypropylene melts: isothermal WAXS experiments with synchrotron radiation," *Elsevier Polymer,* vol. 34, no. 15, pp. 3168-3172, 1993.

[90] B. Monasse, "Polypropylene nucleation on a glass fiber after melt shearing," *Journal of Materials Science,* vol. 27, pp. 6047-6052, 1992.

[91] J. Varga and J. Karger-Kocsis, "Rules of Supermolecular Structure Formation in Sheared Isotactic Polypropylene Melts," *Journal of Polymer Science: Part B Polymer Physics,* vol. 34, pp. 657-670, 1996.

[92] M. Gahleitner, "Propylene–Ethylene Random Copolymers: Comonomer Effects on Crystallinity and Application Properties," *Journal of Applied Polymer Science,* vol. 95, p. 1073–1081, 2005.

[93] M. Etcheverry and S. E. Barbosa, "Glass Fiber Reinforced Polypropylene Mechanical Properties: Enhancement by Adhesion Improvement," *Materials,* vol. 5, pp. 1084-1113, 2012.

[94] B. Monasse and J. Haudin, "Growth Transition and Morphology change in Polypropylene," *Colloid & Polymer Science,* vol. 263, pp. 822-831, 1985.

[95] H. An, X. Li, Y. Geng, Y. Wang, X. Wang, L. Li, Z. Li and C. Yang, "Shear-

Induced Conformational Ordering, Relaxation, and Crystallization of Isotactic Polypropylene," *The Journal of Physical Chemistry B,* vol. 112, p. 12256–12262, 2008.

[96] E. Devaux and B. Chabert, "Nature and origin of the transcrystalline interphase of polypropylene/glass fiber composites after a shear stress," *Polymer Communications,* vol. 32, no. 15, pp. 464-468, 1991.

[97] J. Thomason and A. Van Rooyen, "Transcrystallized interphase in thermoplastic composites, Part I, Influence of fibre type and crystallization temperature," *Journal of Materials Science,* vol. 27, pp. 889-896, 1992.

[98] S. Nagae, Y. Otsuka, M. Nishida, T. Shimizu, T. Takeda and S. Yumitori, "Transcrystallization at gllass fibre/polypropylene interface and its effect on the improvement of mechanical properties of the composites," *Journal of Materials Science Letters,* vol. 14, pp. 1234-1236, 1995.

[99] A. Ziabicki and G. C. Alfonso, "A simple model of flow-induced crystallization memory," *Macromolecular Symposia,* vol. 185, pp. 211-231, 2002.

[100] L. E. Alexander, E. Burke, B. Chalmers and J. A. Krumhansl, "X-ray Diffraction Methods in Polymer Science," *Wiley-Interscience,* 1969.

[101] A. D. Bank, "http://athas.prz.edu.pl/".

[102] K. Jeon, Y. L. Chiari and R. G. Alamo, "Maximum Rate of Crystallization and Morphology of Random Propylene Ethylene Copolymers as a Function of Comonomer Content up to 21 mol %," *Macromolecules ,* vol. 41, pp. 95-108, 2008.

[103] C.-M. Wua, M. Chena and J. Karger-Kocsis, "The role of metastability in the micromorphologic features of sheared isotactic polypropylene melts," *Elsevier Polymer,* vol. 40, p. 4195–4203, 1999.